

**ANALYSIS OF A FSO LINK FOR DIFFERENT MODULATION SCHEME
UNDER VARIOUS TURBULENCE CONDITIONS**

by

Nazia Mehnaz

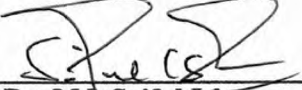
MASTER OF SCIENCE
IN
INFORMATION AND COMMUNICATION TECHNOLOGY



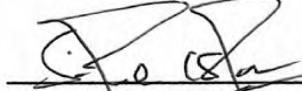
Institute of Information and Communication Technology
BANGLADESH UNIVERSITY OF ENGINEERING AND TECHNOLOGY
September 2019

The thesis titled “ANALYSIS OF A FSO LINK FOR DIFFERENT MODULATION SCHEME UNDER VARIOUS TURBULENCE CONDITIONS” submitted by Nazia Mehnaz, Roll No. 1015312029 and Session: October 2015, has been accepted as satisfactory in partial fulfillment of the recruitment for the degree of Master of Science in Information and Communication Technology on 21 September 2019.


BOARD OF EXAMINERS

1. 


Dr. Md. Saiful Islam
Professor
IICT, BUET, Dhaka. **Chairman
(Supervisor)**

2. 


Dr. Md. Saiful Islam
Director
IICT, BUET, Dhaka. **Member
(Ex-officio)**

3. 

Dr. Md. Rubaiyat Hossain Mondal
Associate Professor
IICT, BUET, Dhaka. **Member**

4. 

Dr. Hossen Asiful Mustafa
Assistant Professor
IICT, BUET, Dhaka. **Member**

5. 

Dr. Mohammed Moseur Rahman
Assistant Professor
East West University, Dhaka. **Member
(External)**

DECLARATION

It is hereby declared that this thesis or any part of it have not been submitted elsewhere for the award of any degree or diploma.

Signature of the Candidate

Nazia Mehnaz

Nazia Mehnaz

DEDICATION

**THIS THESIS IS DEDICATED
TO
MY PARENTS**

ACKNOWLEDGEMENTS

All praises are for the almighty Allah for giving me the strength, without which I couldn't afford to attempt this research work.

I would like to express my sincere and heartiest gratitude to my honorable thesis supervisor **Dr. Md. Saiful Islam**, Professor, Institute of Information and Communication Technology (IICT), Bangladesh University of Engineering and Technology (BUET), Dhaka for his continuous motivation, guidance and keen encouragement which helped me throughout the time of my research work. Nothing is comparable to his keen advice and the freedom he provided for me in research. I am grateful to him for his cooperation throughout my thesis work. My thesis was funded by ICT division, Bangladesh.

I would like to thank all the members of the board of examiners for their precious time in understanding my work and their insightful comments. I would like to thank to all of my friends and colleagues for their cooperation. Finally yet importantly, I am grateful to my family members for their continuous supports and cooperation.

ABSTRACT

Currently, the technologies used in access network include the copper and coaxial cable, optical fiber, wireless internet access and broadband radio frequency. These technologies, in particular copper/coaxial cables and RF based have limitations such as congested spectrum, a lower data rate, an expensive licensing, security issues, etc. With the rapid development and maturity of optoelectronic devices, license free operation and easy installation, free space optical (FSO) communication became a viable alternative for addressing the last mile bottleneck and meets the increasing bandwidth demand of emerging applications and end users. The free-space medium is utilized by FSO system for the transmission of data. As a result, the FSO communication faces challenges from atmospheric channel turbulence or turbidity resulting signal scattering, absorption, temporal and spatial fluctuation of light intensity, which ultimately degrade the link performance substantially. In the last one decade, many research works were carried out to mitigate and improve the performance of FSO link. Advanced data modulation formats can compensate the transmission impairments of the atmospheric turbulence and enhance link sustainability significantly. Generally, most commercially deployed FSO systems uses the intensity modulation direct detection (IM/DD) technique for simplicity but the coherent detection scheme assures higher receiver sensitivity than IM/DD. In this research work, the performance of a FSO link will be evaluated using coherent detection scheme for different modulation formats under various atmospheric turbulence conditions. The performance will be evaluated in terms of signal to noise ratio (SNR) and bit error rate (BER). The modulation techniques used in the analysis are OOK, BPSK, DPSK and QPSK. To evaluate the system error performance in turbulence regimes from weak to strong, the probability density function (pdf) of the received irradiance after traversing in the atmosphere is modeled using the gamma-gamma distribution. In the study, it is found that BPSK gives best BER performance in the proposed system in different turbulence strength compared to any other modulation technique.

TABLE OF CONTENTS

DECLARATION	iii
DEDICATION	iv
ACKNOWLEDGEMENTS	v
ABSTRACT	vi
LIST OF FIGURES	x
LIST OF TABLES	xii
LIST OF ABBREVIATIONS	xiii
LIST OF SYMBOLS	xiv
CHAPTER 1	1
INTRODUCTION	1
1.1 Overview	1
1.2 Motivation of the thesis	2
1.3 Literature review	3
1.4 Objective of the thesis	7
1.5 Main contributions of the thesis	8
1.6 Outline of the thesis	8
CHAPTER 2	10
FREE SPACE OPTICAL SYSTEM	10
2.1 Overview	10
2.2 Introduction To Free Space Optical Communication	10
2.3 Detailed Discussion of Free Space Optical System	11
2.3.1 Transmitter	11
2.3.2 Channel Models	11
2.3.2.1 Lognormal Model	12
2.3.2.2 Negative exponential Model	13
2.3.2.3 K channel Model	14
2.3.2.4 Gamma-Gamma Model	15
2.4 Receivers	16
2.4.1 Photodetectors	16
2.4.2 Photo Detection Noises	18
2.5 Challenges of an FSO communication system	22

2.5.1 Atmospheric Turbulence	22
2.5.2 Refractive index variation	23
2.5.3 Scintillation	24
2.5.4 Pointing error/ jitter	24
2.5.5 Rain	24
2.5.6 Fog	25
2.6 Solutions to the challenges of FSO systems	26
2.7 Summary	27
CHAPTER 3	28
MODULATION AND DETECTION TECHNIQUES	28
3.1 Overview	28
3.2 Types of Modulation Schemes	28
3.3 Selection Criterion of Modulation Scheme	29
3.3.1 Power Efficiency	30
3.3.2 Bandwidth Efficiency	30
3.4 Modulation Schemes used in FSO Channel	31
3.4.1 On-Off keying	32
3.4.2 Pulse Position Modulation	33
3.4.3 Digital Phase Modulation Techniques	34
3.4.4 QAM	38
3.4.5 OFDM FSO System	39
3.5 Detection Techniques in a FSO System	40
3.5.1 Direct Detection	41
3.5.2 Coherent Detection	42
3.5.2.1 Heterodyne Detection	43
3.5.2.2 Homodyne Detection	45
3.6 Summary	46
CHAPTER 4	47
PROPOSED COHERENT FSO SYSTEM AND PERFORMANCE ANALYSIS	47
4.1 Overview	47
4.2 Description of the proposed coherent FSO system	47
4.2.1 Analytical Model	47
4.2.2 Channel Model	49
4.2.3 Modulation Techniques Used in the Analysis	50

4.3 Results and Discussion	52
4.4 Comparison of the proposed FSO system with other FSO system	62
4.5 Summary	62
CHAPTER 5	63
CONCLUSION AND FUTURE WORK	63
5.1 Overview	63
5.2 Summary of the findings of the thesis	63
5.3 Future Work	64

LIST OF FIGURES

Figure 1-1 Typical FSO system.....	2
Figure 2-1: Block diagram of a FSO communication system.....	10
Figure 2-2 Lognormal PDF for different turbulence strength.....	13
Figure 2-3 Negative exponential pdf for different values of I_0	14
Figure 2-4 Gamma-Gamma PDF for different turbulence strength.....	16
Figure 2-5 Diagram of a front-end photodiode detector along with channel impairments	19
Figure 3-1 Transmitted waveforms for OOK: (a) NRZ and (b) RZ ($\lambda = 0.5$).....	32
Figure 3-2 Time waveforms for PPM.....	32
Figure 3-3: 16-QAM constellation diagram.....	37
Figure 3-4 : Block diagram of a FSO system using IM/OOK and APD receiver.....	40
Figure 3-5: Block diagram of a direct detection Receiver.....	41
Figure 3-6: Block diagram a coherent detection scheme.....	42
Figure 4-1: Block diagram of a coherent FSO system.....	47
Figure 4-2: Gamma-Gamma PDF for different turbulence strength	53
Figure 4-3: Comparison of BER performance as a function of average SNR for $\sigma_R^2 = 0.2$	54
Figure 4-4: Comparison of BER performance as a function of average SNR for $\sigma_R^2 = 1$	55
Figure 4-5: Plots of BER vs. SNR for different modulation technique for $\sigma_R^2 = 3$	55
Figure 4-6: Plots of BER vs. Received optical power for different modulation technique.....	56

Figure 4-7: Bit rate vs. Bandwidth for different modulation techniques.....	57
Figure 4-8: Plots of BER vs average SNR for BPSK and QPSK for different turbulence strength.....	58
Figure 4-9: BER performance of BPSK for different turbulence strength.....	59
Figure 4-10: Plots of BER vs Received optical power for BPSK for different turbulence strength.....	59
Figure 4-11: BER performance of BPSK for different values of Rytov variances and link distances.....	60
Figure 4-12: BER performance of BPSK for fixed link distance and different values of Rytov variances.....	61

LIST OF TABLES

Table 2-1 Major challenges in implementation of FSO.....	26
Table 4-1 Simulation parameter of the proposed coherent FSO system	52
Table 4-2 Values of Rytov variance for different link length (L) for a fixed $C_n^2=10^{-13}m^{-2/3}$	60
Table 4-3 Values of Rytov variance for different C_n^2 and link length (L) =1000m.....	61
Table 4-4 Comparison Table of the proposed coherent FSO system with other systems	62

LIST OF ABBREVIATIONS

BER	Bit Error Rate
FSO	Free Space Optical
SNR	Signal to Noise Ratio
LASER	Light Amplification by Stimulated Emission of Radiation
IM-DD	Intensity Modulation Direct Detection
LD	Laser Diode
LOS	Line of Sight
OOK	On-off Keying
OWC	Optical Wireless System
OLO	Optical Local Oscillator
PPM	Pulse Position Modulation
QAM	Quadrature Amplitude Modulation
QPSK	Quadrature Phase Shift Keying
BPSK	Binary Phase Shift Keying
DPSK	Differential Phase Shift Keying
OBPF	Optical Band Pass Filter
FOV	Field of View

LIST OF SYMBOLS

B	Receivers Bandwidth
C_n^2	Refractive index structure parameter
I_0	Mean radiance
$K_0(\cdot)$	Modified Bessel function of order zero
$i_p(t)$	Output current of the photodetector
P_r	Power of the received signal

P_T	Total power of the received signal and the
	local oscillator
$p(I)$	Probability density function of the
	irradiance I
R	Detectors Responsivity
R_L	Load Resistance of the Receiver
σ_n^2	Noise Variance at the output of the
	Receiver
σ_R^2	Rytov variance

CHAPTER 1

INTRODUCTION

1.1 Overview

FSO communication systems have been developed for the growing demand for bandwidth demand in mobile communication. The technology is useful where the installation of buried fiber optic cable to provide a high-speed network is impractical. FSO systems support diverse applications such as satellites, aircrafts, deep-space probes, ground stations and can be used as last mile solutions for efficient deployment in densely populated urban areas or in unstructured environment such as disaster prone areas. FSO communication have gained sufficient interest in recent years as a serious alternatives to radio frequency (RF) links for effectively transferring data at high rates over short distances. In order to provide LOS communication, the transmitter and receiver are placed on high-rise buildings separated by several hundred meters FSO is achieving popularity due to its advantage over RF communication which includes immunity to electromagnetic interference, high data rate, low power consumption, more compact equipment, less cost and low BER[1-2].

FSO technology can provide data rates from hundreds of Mbps to several Gigabits and commercially available systems reports data rates as high as 100 Mbps to 2.5 Gbps [3]. It can be extended upto 10Gbps in WDM based FSO systems. Spectrum congestion in RF systems increases the bandwidth requirement exponentially, which is the biggest challenge in expansion of network. The most efficient solution of the problem would be deploying FSO systems, which guarantee abundant bandwidth. FSO systems operate in infrared range of spectrum. FSO systems can function over a distances of several kilometers as long as there is a clear line of sight (LOS) between the source and the destination with enough transmitter power. FSO operates around 850 nm to 1550 nm wavelengths. The wavelength of 1550 nm is preferred because of more eye safety and reduced solar background radiation [4].

The FSO link comprises of transmitter, atmospheric channel and the receiver. *Figure 1-1* shows a typical FSO system. The transmitter in the FSO link is used to transmit information signal in free space by modulating the electrical information signal into optical signal. The optical signal travels through free space which is captured by the receiver and is converted into an electrical signal [1-4]. The strength of the received signal is one of the performance parameter of a FSO system which is affected by different atmospheric conditions as the signal propagates through the free space. Use of advanced modulation technique can improve a FSO link performance which is affected by the impairments caused by atmospheric turbulence.

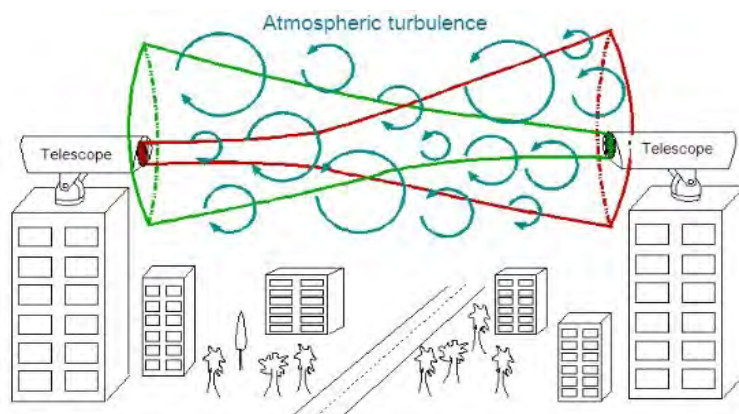


Figure 1-1: A typical FSO system

1.2 Motivation of the thesis

FSO communications can be a key building block for future wide-area wireless data networks and can have great potential for applications in fifth-generation (5G) wireless systems. Such systems are currently being deployed and will encompass a number of complementary access technologies with higher channel capacities, multiple antennas, and Gbit/s data rates. The growth of communications networks has accelerated last-mile access needs for high speed links. Free Space Optics is now a viable choice for connecting the LAN, WAN, and MAN as well as carrying voice, video and data at the speed of light. It is moving closer to being a realistic alternative to laying fiber to the access network. The free-space medium is utilized by FSO system for the transmission of data. As a result, atmospheric conditions inherently affect the transmission, among which turbulence has the most significant effect [5]. It affects the propagation of optical beam

by fluctuation of refractive index due to temperature, pressure and wind variation. Turbulence causes phase shift of propagating optical signals causing distortions in wave front as well as causes intensity distortion, which is termed as scintillation. It also greatly reduces the receiver sensitivity and detection efficiency that results in the degradation of link performance. It is always an interesting problem to analyze the degradation of signal strength due to scintillation of optical signals as well as link performance against atmospheric turbulence channel[6,7]. Many researchers have intensively researched and analysed several implementation techniques of FSO to improve the link performance. Many modulation formats are used in FSO[8].The ability of OOK to resist atmospheric turbulence modulation is particularly weak. Phase modulation techniques have higher sensitivity and excellent properties that is better suited for FSO system. These modulation techniques are also spectrally efficient. Advanced data modulation schemes can compensate the transmission impairments caused by atmospheric turbulence and enhance link sustainability significantly. Most commercially deployed FSO system uses direct detection technique (IM/DD) for simplicity but coherent detection technique ensures more receiver sensitivity as well as link performance. In our research work, we tried to implement a coherent FSO link whose performance is evaluated in terms of SNR and BER for different modulation techniques.

1.3 Literature Review

FSO communication is becoming very popular for transferring data at high rates effectively over short distances. As line of sight (LOS) is the prerequisite of FSO communication, the transmitter and receivers are placed on high rise buildings separated by several hundred meters even kilometres. FSO has number of merits over its demerits: it is lightweight, easily deployable and provides high data rate without any requirement of licensing. Wireless communications have beneficial properties not found in wired communications, such as the lower deployment cost due to the lack of having to dig and lay down cables, ease of construction of network topology, flexible maintenance of operating networks, and soon. Wireless communications also allow users of mobile devices to access the internet at any time and many locations. For instance, IEEE802.11 (Wi-Fi), Bluetooth, and IrDA are intended for short-range wireless data communications, while Long-Term Evolution (LTE) is for long-range wireless communication for both mobile phones and data terminals [1-3]. In some cases, FSO is seen as an

alternative to existing technologies, such as radio frequency. In other cases, FSO is considered as a strong candidate to complement and integrate with next-generation technologies, such as 5G wireless networks. Chen et al. realize a 160 Gbps WDM FSO link using sixteen 10 Gbps channels with OOK modulation technique and a distance of 2.4 km [4].

Traditionally, wireless technology has always been associated with RF technology but transmission with FSO communication technology can be more advantageous in some applications. Spectrum congestion in RF systems face an exponential increase in bandwidth requirement around the globe and it is one of the biggest challenges in expansion of the network. The most efficient solution is the use of FSO system which guarantees abundant bandwidth up to 2000 THz, which is as high as 10^5 times greater than current RF networks [5].

The greatest challenge that FSO faces is the dependence of performance on the atmospheric channel. Different atmospheric conditions like snow, fog, rain, etc. resulting in signal scattering, absorption and fluctuation. When the light beam travels across the atmosphere, it comes across huge attenuation due to which a huge amount of data loss takes place. Atmospheric conditions prominently affect the performance of a FSO system making them highly susceptible to the degrading effects of atmospheric turbulence and pointing errors [6]. Aerosol scattering effects are caused by rain, fog, snow which ultimately reduce the link performance of the FSO system [7,8]. Consequently the optical radiation traversing the turbulent atmosphere experiences random variation/fading in its irradiance (scintillation) and phase. In comparison, when the link range is beyond 1 km, scintillation may severely impact the performance of FSO communication systems resulting in communication link deterioration, i.e., an increase in the error probability in the received signal [9]. FSO system can reach data rates between tens of Gbps to 1 Tbps. Increasing the channel capacity up to 1 Tbps poses the question for the availability of FSO systems. Two main problems, however, have hampered the practical deployment of wireless optical networks. The first problem is atmospheric turbulence, which makes link quality unreliable. Atmospheric turbulence affects the propagation of optical signals, leading to degraded performance directly under various forms such as SNR (Signal-to-

Noise Ratio), BER (Bit Error Rate), outage frequency, and so on. The second problem involves the PAT (Pointing, Acquisition, and Tracking) technique, which is extremely important in FSO systems because of its unguided narrow beam propagation through free space [10,11].

Since an FSO transmitter is highly directional, FSO systems are often designed with a divergence of a few milliradians or less in order to concentrate the optical energy at a receiver. Each “optical transceiver” must be simultaneously pointed at each other for communication to take place. Because of its narrow beam property, precise alignment of the beams is required and PAT is non-trivial even for stationary nodes. Maintenance of an apparent Line of Sight (LOS) between transmitter and receiver end is the main confront to set up communication through FSO technology especially in the troposphere. Because of attenuation caused by atmospheric conditions, the range and the capacity of wireless channels are degraded thereby restricting the potential of the FSO link by limiting the regions and times. The effect of transmitter pointing error in OWC at 850nm and 1550nm are analysed in Optisystem 13.0 software on intersatellite link [12].

Atmospheric turbulence causes the most important impairment in the system performance. It causes the random fluctuation of phase and intensity of the received signal known as channel fading. Intensity fluctuation caused by channel fading leads to an increase in system bit error rate (BER) [13,14]. A number of statistical models have been proposed to describe the channel fading due to weak and strong turbulence. In this respect, Log-normal model has been proved accurate for weak turbulence, the Gamma-Gamma and I-K distribution for both weak and strong turbulence, while the K and the negative exponential distribution are suitable for strong turbulence [15,16,17]. It was shown in [17] that the *K*-distributed turbulence model provides good agreement with experimental data in a variety of FSO experiments involving radiations scattered by strong turbulence. Gamma-gamma distribution shows excellent agreement with all ranges of turbulence if no spatial diversity techniques applied to it [18].

In order to exploit the remarkable bandwidth of FSO technology, it is required to properly characterize the influence of various weather conditions and to use the different optical windows of transmission to mitigate the effects of increasing signal attenuation. In [19], three optical transmission windows are considered that are 850 nm, 1310 nm and 1550 nm

each having their own advantages. Equipments operating on 850 nm wavelength are usually cheaper than equipments operating at higher wavelengths. The window at 1310nm has zero group velocity dispersion. At 1550nm, the loss of optical fiber is minimum that is 0.2 dB/km. Low loss means the distance between the repeater and optical amplifier can be large. 1550nm is also a eye safe wavelength. The short wavelength infrared spectrum (1500nm-1600nm) is well applicable for FSO link [16]. This wavelength laser is generally preferred because it provides large range, long life and high data rate. In 2008 MRV communication has introduced FSO based telescope TS- 10GE system with 10 Gbit/s data rate at distance 350m . Now presently research by MOSTCOM company in 2013 invent Artolink M1-10G with high data rate 10 Gbit/s and their distance up to 2.5 Km. In outer space range of FSO communication is currently 10^6 using telescope [21].

In order to mitigate the effect of atmospheric turbulence, the researchers across the world have carried out a large number of laser atmospheric propagation experiments and researches. Different methods have been proposed such as coherent optical modulation, coded modulation technology, multiple input multiple output (MIMO) system, WDM FSO links, larger aperture receiver technology, OFDM RF-FSO system, etc. [22-28].

FSO communication links can potentially benefit from the simultaneous transmission of multiple spatially orthogonal beams through a single aperture pair, such that each beam carries an independent data stream and the total capacity is multiplied by the number of beams. Orthogonality of the beams enable efficient multiplexing and demultiplexing at the transmitter and receiver, respectively. An optical beam can carry orbital-angular-momentum (OAM), and such OAM has gained interest for its potential in achieving efficient multiplexing of multiple data-carrying beams [29].

Most commercially deployed FSO system usually uses IM/DD method but coherent detection technique gives better BER performance. The coherent receiver uses a local oscillator which increases the receiver sensitivity as well as better BER vs. SNR performance [30]. In Ref. [31], a performance analysis for intensity modulation-direct detection (IM-DD) FSO systems over gamma-gamma turbulence channels were presented. For a coherent FSO systems, Refs. [32] proposed alternative implementations enabling a higher receiver sensitivity than that of IM-DD, especially when the power of the

local oscillator laser is sufficiently high. Moreover, a good modulation technique along with coherent receiver can improve a FSO systems performance to a great extent [33-36].

Optical field has three physical attributes (intensity, phase and polarization) which can be used to transmit information. Considering that the atmospheric turbulence mainly affects on the light intensity, pulse-position modulation (PPM) [37] is commonly used in FSO communication. However, PPM is a power efficient modulation technique but it is prone to slot synchronization error [38]. Since fiber-optic technologies have been well developed and fiber-optic networks have been widely deployed from the local access networks to the long-haul intercontinental networks. Some commonly used modulation formats in fiber-optic transmission system, including on-off keying (OOK), Differential phase-shift keying (DPSK) [39], Binary phase-shift keying (BPSK), Quadrature phase-shift keying (QPSK) have also been investigated in FSO systems but the detection technique was not coherent [38-40].

Simplicity is the advantage of OOK, while in PSK format, which encodes information on its phase, can mitigate the severe effect of scintillation to some extent. Compared with the binary format such as OOK and DPSK, the Quadrature Phase Shift keying (QPSK) format doubles spectral efficiency by taking advantage of the two signal quadratures of an optical carrier. Thus, 2 information bits are transmitted per symbol, being represented by four possible optical phase variations between successive symbol periods [41]. Although QPSK is spectrally efficient, BPSK and QPSK gives almost similar power efficiency. The receiver circuit arrangement of BPSK format is simpler than QPSK [42,43]. Therefore there is a need to design a FSO system where the detection technique is coherent and different modulation formats can be applied too.

1.4 Objectives of the Thesis

The objective of this research work is to provide analytical technique to evaluate the performance of a FSO link for different turbulence conditions and modulation schemes. The main objectives are:

- i. To develop an analytical model for a coherent FSO link with different modulation schemes considering the atmospheric channel.

- ii. To evaluate the SNR and BER performance of the FSO link under various turbulence conditions using the developed analytical model.

1.5 Main Contributions of the Thesis

A generalized analytical model for FSO link is developed assuming coherent detection. Gamma-Gamma atmospheric channel model is used for strong and weak turbulence due to the presence air pocket, moving currents, rain, fog, etc. Four modulation techniques: OOK, BPSK, QPSK, DPSK are used to analyze the proposed model. The system is analyzed from weak to strong turbulence regime for all the modulation schemes to find the best scheme for the model. It is shown in the research work that BPSK gives better performance than the other modulation schemes.

The findings of this research may be incorporated in the design of a FSO link in the presence of both strong and weak turbulence. For evaluating the performance of the FSO link, the numerical simulation will be done using MATLAB. The FSO link performance will also be observed in terms of signal to SNR, BER and other metrics for the different modulation techniques stated above. It is expected that FSO transmission quality and reliability will be increased significantly.

1.6 Outline of the Thesis

The thesis is organized as follows:

Chapter 2 provides the detailed discussion of free space optical system with block diagram. A brief discussion is provided on the transmitter, receiver, channel model used in a FSO communication system. Also, the detection techniques used in FSO is discussed in this chapter.

Chapter 3 presents different modulation and detection techniques used in Free Space optical communication systems.

Chapter4 presents the analytical approach that is developed for a coherent FSO link and the link performance is evaluated under different turbulence condition and for different modulation schemes like OOK, BPSK, DPSK, QPSK. The link is analyzed more with the BPSK modulation scheme as it provides the best performance among the four modulation techniques.

Chapter 5 focuses on the outcome of the thesis and summarises the achievement and findings of the research work. The scope of the future research work that can be carried is described in the chapter.

CHAPTER 2

FREE SPACE OPTICAL SYSTEM

2.1 Overview

The detailed description of free space optical wireless system is provided in this chapter with the details of transmitter and receiver side of a FSO system. Different atmospheric models used in FSO systems are also discussed. The challenges of FSO system are also addressed in this chapter.

2.2 Introduction To Free Space Optical Communication

A free space optical communication refers to line of sight communication link between communicating node separated by atmosphere as unguided medium between them. The main requirement for FSO link is line of sight condition between two FSO units. Each unit consists of an optical transceiver with a laser transmitter and a receiver to provide full duplex (bi-directional) capability. Each FSO unit uses a high-power optical source (i.e Laser, LED) and the network traffic is converted into light pulses. A lens in the transmitter transmits light through the atmosphere to another lens receiving the information. The received signal is converted back to digital signal and connected to the network[1]. *Figure 2-1* shows the basic block diagram of a FSO system.

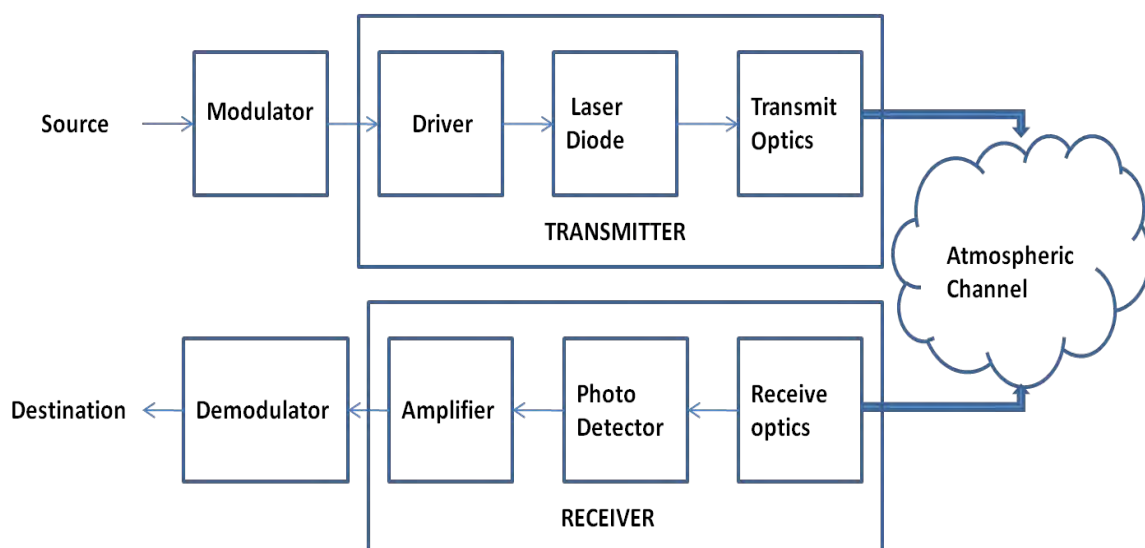


Figure 2-2: Block diagram of a FSO communication system

The data to be transmitted can be modulated using intensity, phase or frequency characteristics of the optical carrier beam that lies in the infrared and visible part of the spectrum corresponding to the wavelengths between 850nm and 1550nm [9].

2.3 Detailed Discussion of Free Space Optical System

In this section, the each part of an FSO system has been discussed.

2.3.1 Transmitter

On the transmitting side, the transmitter consists of data source, modulator, driver, LD source and transmit optics. Lasers, because of their directional beam profile, are most commonly employed for outdoor applications like FSO communication. For the application, light source adopted must have the appropriate wavelength, line width, numerical aperture, high radiance with a small emitting surface area and high modulation bandwidth. The LD source small size, low forward voltage and drive current, excellent brightness in the visible wavelength and with the option of emission at a single wavelength or range of wavelengths. Usually, FSO uses the infrared (IR) part of spectrum which is the short-wavelength infrared (1530nm-1560nm)[1] .

2.3.2 Channel Models

As the optical signal propagates through the atmospheric channel, it encounters variation in the intensity of the signal due to various unpredictable environmental factors like fog, rain, snow, etc. Other factors responsible for degrading the quality of the optical beam in FSO communication are absorption and scattering, beam divergence loss, free-space loss, and pointing loss. Also, turbulence in the atmosphere causes random fluctuations in the intensity and phase of the received signal. Atmospheric turbulence causes significant impairments in the performance of a FSO channel. The reliability of the designed optical communication link will depend on the accurate estimate of the random fluctuation in the signal or in other words on the probability density function (pdf) of this random irradiance signal. There are many pdf models proposed for both weak and strong turbulence[6]. The atmospheric turbulence impairs the performance of a FSO link by causing the received optical signal to vary randomly thus giving rise to signal fading. The fading strength depends upon the link length, the wavelength of the optical radiation and the refractive index structure parameter C_n^2 of the channel. From practical point of view, it

is desirable to have a tractable pdf model for irradiance fluctuation so that we can predict the performance of the link with an acceptable accuracy and the channel is characterized by Rytov variance σ_R^2 . The turbulence induced fading is weak when $\sigma_R^2 < 1$ and this defines the limit of validity of the model.

$$\sigma_R^2 = 1.23 C_n^2 k^{7/6} L^{11/6} \quad (0)$$

C_n^2 is the refractive-index structure parameter and its value ranges from 10^{-13} to 10^{-17} , k is the wave number and L is the distance between transmitter and receiver.

The pdf's proposed for these channels for different degree of turbulence are [10]:

1. Log-normal
2. Negative exponential
3. K channel model
4. Gamma-Gamma

Log-normal distribution is the most commonly used model for the probability density function of the irradiance for weak turbulence condition. But, Log-normal pdf underestimates the behavior in the tails as compared with the measured data. In high turbulence conditions, there are multiple scattering effects, which become important. These cannot be accounted accurately with Log-normal pdf which significantly affects the accuracy of the estimated performance at high turbulence. The negative exponential model on the other hand models high turbulence effects well. The rest two distribution have the irradiance modeled as a result of two multiplicative random process. Gamma-gamma is a two-parameter distribution based on a double stochastic theory and can model both the weak and strong turbulence condition. In the following section, the pdf models will be discussed in detail.

2.3.2.1 Lognormal Model

Lognormal distribution is widely used model for the probability density function (pdf) of the irradiance due to its simplicity in terms of mathematical calculation. This turbulence model is only applicable to weak turbulence conditions and for propagation distances less than 100 m [8]. Considering lognormal model, the pdf of the received optical field I is given as $f(I)$:

$$f(I) = \frac{1}{\sqrt{2\pi\sigma_R^2}} \exp\left(-\frac{\left(\ln\left(\frac{I}{I_0}\right) + \frac{\sigma_R^2}{2}\right)^2}{2\sigma_R^2}\right), I \geq 0 \quad (0)$$

Where,

I represents the irradiance at the receiver

I_0 is the signal irradiance without scintillation.

Figure 2-2 shows the probability density functions curve of Lognormal model for different turbulence strength.

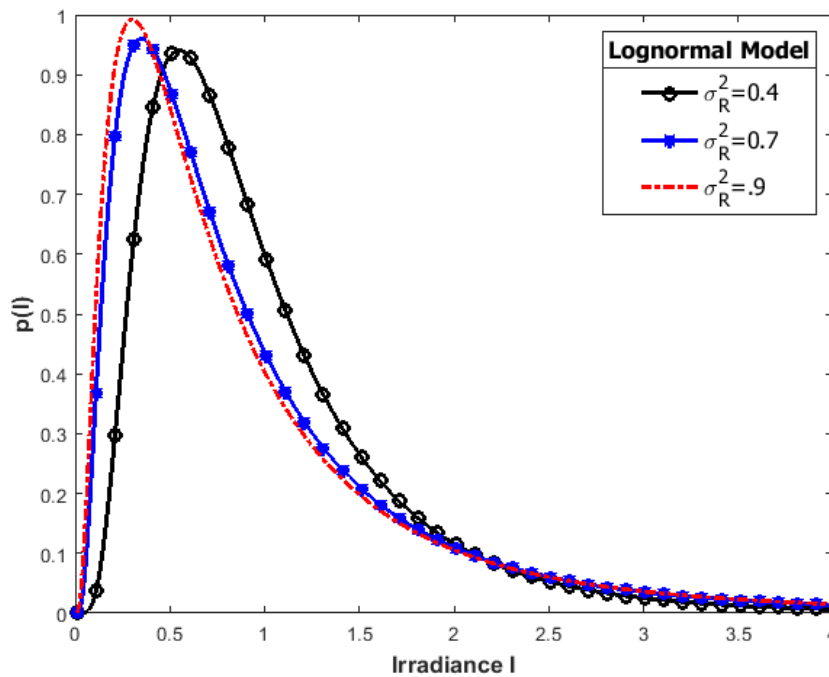


Figure 2-2: Lognormal PDF for different turbulence strength

2.3.2.2 Negative Exponential Model

In case of strong irradiance fluctuations where link length spans several kilometers, number of independent scatter become large. In that case, signal amplitude follows a Rayleigh distribution, which in turn leads to a negative exponential statistics for the signal intensity (square of field amplitude). This is given by [1]:

$$f(I) = \frac{1}{I_0} \exp\left(-\frac{I}{I_0}\right), I \geq 0 \quad (0)$$

Here, I_0 is the mean radiance (average photon count per slot).

where $E[I] = I_0$ is the mean received irradiance. During the saturation regime, the value of the S.I=1. It is noteworthy that other turbulence models such as the log-normal-Rician and the I-K distributions[9], which are both valid from weak-to-strong turbulence regimes; the K-model, which is only valid for the strong regime, and the gamma-gamma turbulence models all reduce to the negative exponential in the limit of strong turbulence. The negative exponential pdf is shown in *Figure 2-3*.

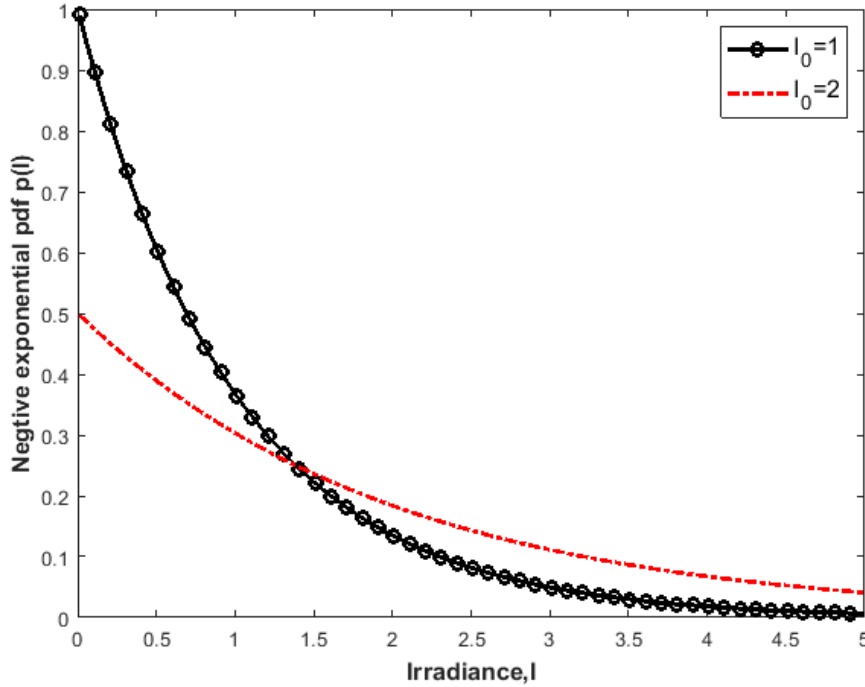


Figure 2-3: Negative exponential pdf for different values of I_0

2.3.2.3 K-channel Model

This statistical model is used in strong turbulence condition. Here, SI is nearly 1 and the value of log intensity variance is between 3 and 4.

This channel model can be considered as a product of two independent models- Exponential and Gamma. This model provides excellent agreement between theoretical and experimental values. Pdf for the instantaneous electrical SNR, γ , at the receiver can be given by[10],

$$P_{\gamma}(\gamma) = \frac{\beta^{\frac{\beta+1}{2}} \gamma^{\frac{\beta-3}{4}}}{\zeta^{\frac{\beta+1}{4}} \Gamma(\beta)} K_{\beta-1} \left(2\sqrt{\beta} \sqrt{\frac{\gamma}{\zeta}} \right) \quad (0)$$

Where β is related to the effective number of discrete scatters, while $\Gamma(\cdot)$ is the Gamma function. $K_{\beta-1}$ is the modified Bessel function of the second kind of order ν . ζ is average electrical SNR at the receiver.

2.3.2.4 Gamma-Gamma Model

Andrews et. al. [7] introduced the modified Rytov theory and proposed gamma-gamma pdf as a useful mathematical model for atmospheric turbulence. This modified Rytov theory defines the optical field as a function of perturbations which are due to large scale and small scale atmospheric effects. The normalized irradiance is given as $I = I_x I_y$ where I_x and I_y arise from large scale and small scale turbulent eddies and each of them follows gamma distribution. This gives the gamma-gamma pdf as [11]:

$$f(I) = \frac{2(\alpha\beta)^{\frac{\alpha+\beta}{2}}}{\Gamma(\alpha)\Gamma(\beta)} I^{\left(\frac{\alpha+\beta}{2}-1\right)} K_{\alpha-\beta}(2\sqrt{\alpha\beta I}) \quad (0)$$

where, $I > 0$ is the received signal irradiance, α and β are the parameters of probability density function, $\Gamma(\alpha); \Gamma(\beta)$ are the Gamma function and K_a is the modified Bessel function of second kind of order a . Here, α and β are the effective number of small scale and large scale eddies of turbulent environment, which are given by :

$$\alpha = \left\{ \exp \left[\frac{0.49 \sigma_R^2}{\left(1 + 1.1 \sigma_R^{\frac{12}{5}}\right)^{\frac{7}{6}}} \right] - 1 \right\}^{-1} \quad (0)$$

$$\beta = \left\{ \exp \left[\frac{0.49 \sigma_R^2}{\left(1 + 1.1 \sigma_R^{\frac{12}{5}}\right)^{\frac{7}{6}}} \right] - 1 \right\}^{-1} \quad (0)$$

where, $\sigma_R^2 = 1.23 C_n^2 k^{7/6} L^{11/6}$ is called the Rytov variance which represents the variance of log-intensity fluctuation. C_n^2 is the refractive-index structure parameter and its value ranges from 10^{-13} to 10^{-17} , k is the wave number and L is the distance between transmitter and receiver. When $\sigma_R^2 < 1$, it means the light intensity fluctuation is weak and $\sigma_R^2 > 1$ means strong intensity fluctuation. The Gamma-Gamma exponential pdf is shown in *Figure 2-4*. This figure is plotted for different turbulence strength and the channel model works well for both weak and strong turbulence regime.

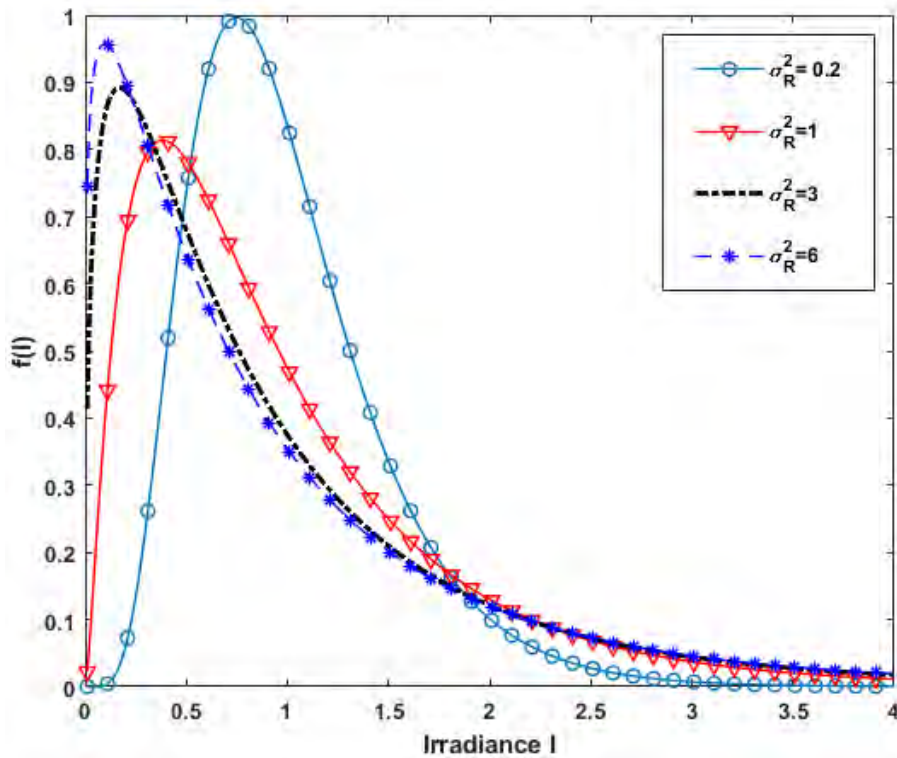


Figure 2-4 Gamma-Gamma PDF for different turbulence strength

2.4 Receivers

On the receiver side of FSO unit, there are receiver optics, photodetectors and amplifiers. At the receiving end, a high directionality telescope is used to collect as much of the transmitted power as possible but also to reduce the background ambient light, which introduces noise thus reduces the link performance. The optical power collected by the telescope strikes the photodetector.

2.4.1 Photodetectors

The photodetector is a square law optoelectronic transducer that generates an electric signal which is proportional to the square of the instantaneous optical field impinging on its surface. Thus, the signal generated by a photodetector is always proportional to the instantaneous received optical power. Since the optical signal is generally weak, having travelled through the communication channel, the photodetectors must therefore meet the stringent performance requirements such as high sensitivity within its operational range of wavelengths, a low noise level and an adequate bandwidth to accommodate the desired data rate. Quantum efficiency is used as a metric to characterize a photodetector.

Numbers of electron-hole pairs generated by photodetectors to the incident photons in a given time is termed as quantum efficiency, η_{qe} .

$$\eta_{qe} = \frac{\text{Electrons out}}{\text{Photons input}}$$

Consider an incoming optical radiation with an average power P_r impinging on a photodetector over period T . Then the electric current generated by the detector is given by [12]:

$$i = \frac{\eta_{qe} \lambda q P_r}{hc} = R P_r \quad (0)$$

where q is the electronic charge and R is the photodetectors responsivity defined as the photocurrent generated per unit incident optical power.

$$R = \frac{\eta_{qe} \lambda q}{hc} = \frac{\lambda}{1.24} \eta_{qe} \quad (0)$$

There are different types of photodetectors that could be used in optical receivers. PIN and APD detectors are most popular and widely used which meet the requirement of high sensitivity and responsivity.

2.4.1.1 PIN Photodetectors

The PIN photodetector consists of p - and n -type semiconductor materials separated by a very lightly n -doped intrinsic region [13]. In normal operating conditions, a sufficiently large reverse bias voltage is applied across the device. For the device to convert an incident photon into an electron/electric current, the energy of the incoming photon must not be less than the band-gap energy of the semiconductor material. The incident photon uses its energy to excite an electron from the valence band to the conduction band, thereby generating a free electron-hole pair in the process. Normally, the incident light is concentrated on the depleted intrinsic region. The high electric field present in this depleted region causes the generated charge carriers to separate and collect across the reverse biased junction. This gives rise to a current flow in an external circuit and there is one electron flowing for every carrier pair generated. The upper cut-off wavelength λ_c , in micrometres (μm) is generally given by Equation below where E_g is the energy bandgap of the semiconductor material in electron-volt (eV).

$$\lambda_c = \frac{hc}{E_g} \quad (0)$$

The operating wavelength ranges for different photodetector materials. The responsivity of a PIN photodetector is always less than unity. PIN photodetectors are capable of operating at very high bit rates exceeding 100 Gbps [12–13].

2.4.1.2 APD Photodetectors

The APD is different from the PIN photodetector, in that it provides an inherent current gain through the process called repeated electron ionization. This culminates in increased sensitivity since the photocurrent is now multiplied before encountering the thermal noise associated with the receiver circuit. Hence, the expression for the responsivity of an APD includes a multiplication (or gain) factor given by-

$$M = \frac{I_T}{I_p} \quad (0)$$

where I_T is the average value of the total output current and $I_p = RPr$ is the primary unmultiplied photocurrent (i.e., PIN diode case).

Thus the responsivity value of an APD can be greater than unity. The APD offers a higher sensitivity than the PIN detector but the statistical nature of the ionization/avalanche process means that there is always a multiplication noise associated with the APD [14]. The avalanche process is also very temperature sensitive. These factors are very important and must always be taken into account whenever an APD is used in an optical communication system.

2.4.2 Photo Detection Noises

The noise sources as well as the frequency and distortion performance of a wireless optical link are decisive factors in determining the link performance. In line with nearly all communication systems, identification of the noise sources at the receiver front end, where the incoming signal contains the least power, is critical. The two primary sources of noise at the input of the receiver are due to shot noise from the received photocurrent and noise from the receiver electronics. *Figure 2-5* illustrates a schematic of a receiver front end with photodetector as well as noise sources indicated. Photogenerated shot noise is a major noise source in the wireless optical link. It arises fundamentally due to the discrete nature of energy and charge in the photodiode. Thermal noise, due to the resistive element, is generated independently of the received optical signal.

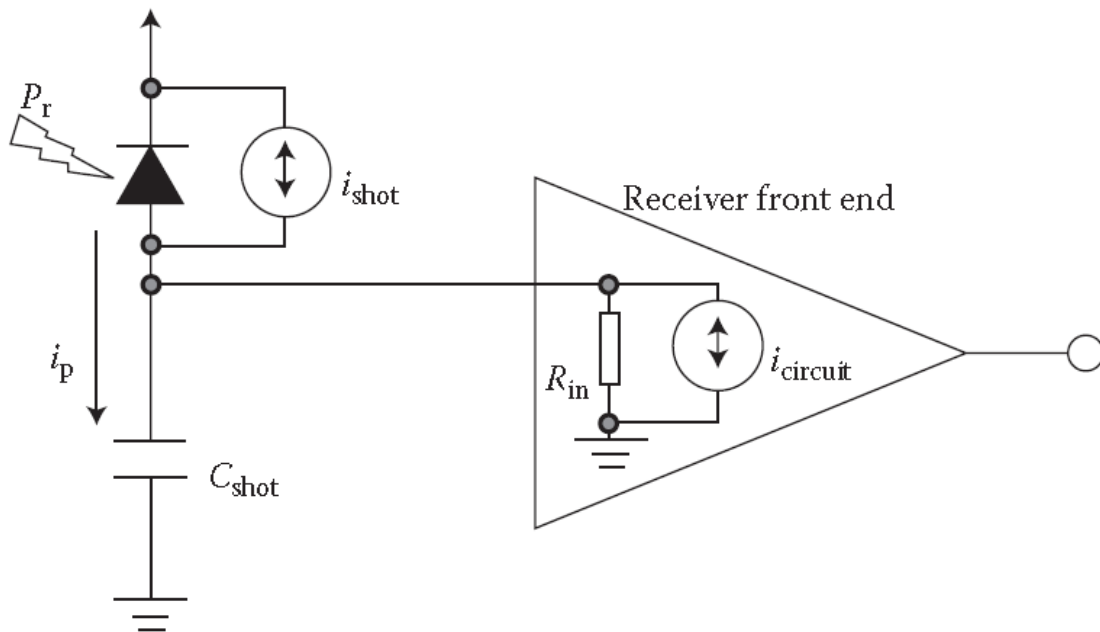


Figure 2-5: Diagram of a front-end photodiode detector along with channel impairments.

The various sources of noise in optical communications are discussed below. For FSO systems, the noise from the background radiation can be significant.

2.4.2.1 Photon Fluctuation Noise

For an ideal photodetector, the only significant noise that affects its performance is that associated with the quantum nature of light itself, the by-product of which is that the number of photons emitted by a coherent optical source in a given time is never constant. Although for a constant power optical source, the mean number of photons generated per second is constant, the actual number of photons per second follows the Poisson distribution. This results in photon fluctuation or quantum noise. Quantum noise (also termed photon noise) is a shot noise that is present in all photon detectors due to the random arrival rate of photons from the data carrying optical source and background radiation.

The quantum fluctuation is also important because it dominates over the thermal fluctuations within the photodetector, since $hf > \kappa T_e$ where h and f are the Planck's constant and the radiation frequency, respectively, while κ and T_e represent

the Boltzmann's constant and temperature, respectively. The quantum noise is a shot noise with variance.

$$\sigma_{q-pin}^2 = 2q \langle i \rangle B \quad (0)$$

$$\sigma_{q-apd}^2 = 2q \langle i \rangle BF M^2 \quad (0)$$

where the bandwidth of the electrical filter that follows the photodetector is represented by B Hz. The shot noise is in fact proportional to $(n_{\text{photon}})^{0.5}$, where n_{photon} is the equivalent number of photons after degradation caused by imperfect conversion due to the quantum efficiency.

For coherent receivers, the shot noise due to the optical signal and the LO is given by-

$$\sigma_{q-CS}^2 = 2q \langle i_s \rangle M^2 B_c \quad (0)$$

$$\sigma_{q-CLO}^2 = 2q \langle i_{lo} \rangle M^2 B_c \quad (0)$$

where B_c is the bandwidth of the coherent receiver.

For the heterodyne case, the LO shot noise is much larger than the signal shot noise; therefore, the signal shot noise can be ignored.

2.4.3.2 Background Radiation

This type of noise is due to the detection of photons generated by the environment. Two types of sources contribute to background radiation (ambient light) noise: localized point sources (e.g., the Sun) and extended sources (e.g., the sky). Background radiation from other celestial bodies such as stars and reflected background radiation are assumed to be too weak to be considered for a terrestrial FSO link; however, they contribute significantly to background noise in deep space FSO. The following are the irradiance (power per unit area) expressions for both the extended and localized background sources [14-15].

$$I_{sky} = N(\lambda) \Delta \lambda \Omega^2 \quad (0)$$

$$I_{sun} = W(\lambda) \Delta \lambda \quad (0)$$

where $N(\lambda)$ and $W(\lambda)$ are the spectral radiance of the sky and spectral radiant emittance of the sun, respectively, $\Delta\lambda$ is the bandwidth of the OBPF that precedes the photodetector and Ω is the photodetector's field of view angle in radians. By carefully choosing a receiver with a very narrow FOV and $\Delta\lambda$, the impact of background noise can be greatly reduced. OBPF in the form of coatings on the receiver optics/ telescope with $\Delta\lambda < 1$ nm are now readily available. Empirical values of $N(\lambda)$ and $W(\lambda)$ under different observation conditions are also available in the literature. The background radiation is a shot noise with variance [15].

For a coherent receiver, use Equation (14) and change B to B_c . In most practical systems, the receiver SNR is limited by the background *shot noise* that is much stronger than the quantum noise and/or by thermal noise in the electronics following the photodetector.

$$\sigma_{bg}^2 = 2qBR(I_{sky} + I_{sun}) \quad (0)$$

2.4.3.3 Thermal Noise

Thermal noise, also known as the Johnson noise, occurs in all conducting materials. It is caused by the thermal fluctuation of electrons in any receiver circuit of equivalent resistance R_L and temperature T_e . The electrons are in constant motion, but they collide frequently with the atoms or molecules of the substance. Every free flight of an electron constitutes a minute current. The sum of all these currents taken over a long period of time must, of course, be equal to zero. The thermal noise is regarded as a 'white' noise. This is because the power spectral density (PSD) is independent of frequency. Moreover, the thermal noise obeys the Gaussian distribution with zero mean and variance for IM-DD and coherent receivers defined by [16]-

$$\sigma_{th-D}^2 = \frac{4kT_e B}{R_L} \quad (0)$$

$$\sigma_{th-CS}^2 = \frac{4kT_e B_c}{R_L} \quad (0)$$

2.4.3.4 Dark Current and Excess Noise

Since the photocurrent is proportional to the incident light power, the photon shotnoise increases with respect to the increase of the incident power (in square root fashion). The lower end of this relation is limited by the noise from the dark current, which is present even when there is no input light. It is produced by the transition of electrons from the valence to the conduction band due to causes other than photoninduced excitation; its magnitude is closely related to the energy band-gap of the photodetector material(s). Large band-gap materials, such as silicon (Si), indium phosphide (InP) and gallium arsenide (GaAs), show very low values of mean dark current, $\langle i_d \rangle$, while for germanium (Ge), the value could be significant when they are operated at room temperature [15]. The dark current is a combination of bulk and surface leakage currents, carries no useful information and thereby constitutes a shot noise whose variances are given by the following-

$$\sigma_R^2 = 1.23 C_n^2 k^{7/6} L^{11/6} \quad (27)$$

$$\sigma_{ds}^2 = 2qI_1B \quad (28)$$

Where, $k = \frac{2\pi}{\lambda}$ is the wave number and I_1 is the detector's primary unmultiplied surface leakagecurrent .

For coherent receivers, the dark current noise is given by [1]-

$$\sigma_{D-C}^2 = 2qI_d M^2 B_c$$

where I_d is the detector's primary unmultiplied dark current .

2.5Challenges of an FSO communication system

The major challenges encountered in the design and implementation of an FSO system are outlined below.

2.5.1 Atmospheric Turbulence

Atmospheric circulation due to distribution of temperature on the surface of earth, wind flowdue to the change of atmospheric pressure and velocity variation generateatmospheric turbulence. Clear air turbulence phenomena affect the propagation ofoptical beam by both spatial and temporal random fluctuations of refractive index due

to temperature, pressure, and wind variations along the optical propagation path. Atmospheric turbulence primarily causes phase shifts of the propagating optical signals resulting in distortions in the wave front and this distortion is referred to as optical aberrations. Atmospheric turbulence also causes intensity distortion, which is referred to as scintillation. Aerosols, moisture, temperature and pressure changes produce refractive index variations in the air by causing random variations in air density. These variations are referred to as eddies or air pockets having a lens effect on light passing through them [17]. The refractive index variation causes phase perturbation of the wave front isophase plane of propagating light. As a result, secondary waves generated from different point of wave front have different phase, and their interference with each other gives amplitude variation. In other words, air pockets will act as lenses for propagating light having different refractive indexes, and they will focus-defocus light randomly. The net result is that, intensity of received optical signal will not be constant but fluctuating randomly similar to the amplitude fading due to multipath propagation in RF wireless communication.

When a plane wave passes through these eddies, parts of it are refracted randomly causing a distorted wave front with the combined effects of variation of intensity across the wave front and warping of the isophase surface. If the size of the turbulence eddies are larger than the beam diameter, the whole laser beam bends. If the sizes of the turbulence eddies are smaller than the beam diameter and so the laser beam bends, they become distorted. Small variations in the arrival time of various components of the beam wave front produce constructive and destructive interference and result in temporal fluctuations in the laser beam intensity at the receiver.

2.5.2 Refractive Index Variation

Refractive index structure parameter (C_n^2) is the most significant parameter that determines the turbulence strength and depends on the geographical location, altitude, and time of day [18]. There is the largest gradient of temperature associated with the largest values of atmospheric pressure and air density close to the ground. Therefore, the value of refractive index structure should be larger at sea level and smaller as the altitude increases, because the temperature gradient decreases with the increase of altitude and so the air density, results smaller refractive index structure. In the horizontal path even over a reasonably long distance, refractive index structure parameter may be assumed to be

practically constant. Value of atmospheric refractive structure parameter depends on channel condition and for terrestrial link. Typical value of refractive index structure parameter for a weak turbulence at ground level can be as little as $10^{-17} \text{ m}^{-2/3}$, while for a strong turbulence it can be up to $10^{-13} \text{ m}^{-2/3}$ or larger. Numbers of parametric models have been formulated to describe the refractive index structure parameter profile and among those, one of the more used models is the Hufnagel-Valley model [18].

2.5.3 Scintillation

Irradiance fluctuation due to atmospheric turbulence is known as scintillation, and σ_i^2 is used to represent scintillation index. This parameter directly indicates strength of atmospheric turbulence and defined as normalized variance of intensity fluctuation which represents as: $\sigma_i^2 = \frac{E[I^2]}{E[I]^2} - 1$ [19]. This scintillation index is directly related to channel parameter and system parameter as: where C_n^2 is atmospheric refractive index structure parameter, $kx = 2\pi/\lambda$ is known as wave number where, λ is the wavelength and L is the link distance in meter. For weak turbulence, $\sigma_i^2 \simeq \sigma_R^2$.

For a constant atmospheric refractive structure parameter, scintillation index is completely dependent on link length L , since wavelength of light is constant. Scintillation is the most noticeable parameter for FSO systems. Light traveling through scintillation will experience intensity fluctuations, even over relatively short propagation distance.

2.5.4 Pointing error/ jitter

In addition to the effects of atmospheric turbulence, FSO links are also highly dependent on the pointing performance. The pointing-error is the deviation between the desired antenna orientation and its current actual position. This error can arise from mechanical misalignment, errors in tracking systems and due to mechanical vibrations present in the system. The pointing error consists of two components: a fixed error, called boresight error and a random error, called jitter. Jitter is superimposed over the fixed boresight error and modeled as a two dimensional random variables [18, 19]. Due to boresight error and jitter, each received intensity sample can be thought of as a randomly sampled point on a random irradiance profile.

2.5.5 Rain

Rain is liquid water in the form of droplets that have condensed from atmospheric water vapour and then precipitated to become heavy enough to fall under gravity. Rain is a major component of the water cycle and is responsible for depositing most of the freshwater on the Earth. The major cause of rain production is moisture moving along three dimensional zones of temperature and moisture contrasts known as weather fronts. If enough moisture and upward motion is present, precipitation falls from convective clouds those with strong upward vertical motion such as Cumulonimbus thunder clouds which can organize into narrow rain band. Rain is unpredictable attenuation and the major impairment to FSO link availability. Attenuation of the rain is independent of the wavelength and it is the function of precipitation intensity [18].

Scattering due to rainfall is called non-selective scattering, because the radius of raindrops are 100-1000 μm is significantly larger than the wavelength of typical FSO systems. The laser is able to pass through the raindrop particle with less scattering effect occurring. The haze particles are very small and stay longer in the atmosphere, but the rain particles are very large and stay shorter in the atmosphere. This is the primary reason that attenuation via rain is less than haze. An interesting point to note is that RF wireless technologies that use frequencies above approximately 10 GHz are adversely impacted by rain and little impacted by fog. This is because of the closer match of RF wavelengths to the radius of raindrops, both being larger than the moisture droplets in fog.

Rain is precipitation of liquid drops with diameters greater than 0.5 mm when the drops are smaller; the precipitation is usually called drizzle. The optical signal is randomly attenuated by fog and rain when it passes through the atmosphere. The main attenuation factor for optical wireless link is fog. However, rain also imposes certain attenuation. When the size of water droplets of rain becomes large enough it causes reflection and refraction. As a result, these droplets cause wavelength independent scattering. Majority of the rain drops belong to this category. The increase in rainfall rate causes linear increase in attenuation, and the mean of the raindrop sizes also increases with the rainfall rate and is in the order of a few mm [19].

2.5.6 Fog

Fog is a cloud of small water droplets near ground level and sufficiently dense to reduce horizontally visibility to less than 100 m. Fog is formed by the condensation of

watervapor on condensation nuclei that are always present in natural air. This can result asoon as the relative humidity of the air exceeds saturation by a fraction of 1%. In highlypolluted air the nuclei may grow sufficiently to cause fog at humidity's of 95% or less. Another way is to use visibility data to predict specific attenuation. The modelsKruse, Kim and Al Naboulsi use this approach and predict specific attenuationusing visibility. The attenuation of 10 μm is expected to be less than attenuation ofshorter wavelengths. Kim rejected such wavelength dependent attenuation for lowvisibility in dense fog. Al Naboulsi and et.al developed simple relations allowing theevaluation of the attenuation in the 690 to 1550 nm wavelength range and for visibilitiesgoing from 50 to 1000 m for two types of fog: advection fog and convection fog.

The advection fog is generated when the warm, moist air flows over a colder surface. The air in contact with the surface is cooled below its dew point, causing thecondensation of water vapour. It appears more particularly in spring when southerndisplacements of warm, moist air masses move over snow covered regions. Theradiation or convection fog is generated by radiative cooling of an air mass during thenight radiation when meteorological conditions are favorable such as very low speedwinds, high humidity, clear sky etc. It forms when the surface releases the heat that isaccumulated during the day and becomes colder: the air which is in contact with thissurface is cooled below the dew point, causing the condensation of watervapor, whichresults in the formation of a ground level cloud. This type of fog occurs moreparticularly in valleys [18,19,20].

2.6 Solutions to the Challenges of FSO systems

The different challenges associated with aFSO system have different impact on the performance of the system. The solution of major challenges encountered in the design and implementation of FSO system is outlined in the following Table 2-1.

Table 2-1 Major challanges in implementation of FSO

	Causes	Effects	Solutions
Intersymbol Interferences (ISI)	Multipath Propagation	Quality of transmission Multipath Distortion or dispersion Reduce data rates	• Equalization and predistortion equalization

			<ul style="list-style-type: none"> • Forward error correction (FEC) • Spread spectrum techniques • Multiple-subcarrier modulation (MSM) • More bandwidth efficient than single-carrier • OFDM, MSM • Multibeam transmitter
Safety	Laser radiation	Damage to eye and skin	Power efficient modulation PPM, DPIM
Turbulence	Random refractive index variation	Scintillation Phase fluctuation Polarization fluctuation	<ul style="list-style-type: none"> • Coding, for example, LDPC, FEC, MIMO • Diversity reception (temporal and spatial) • Adaptive optics • Robust modulation techniques • Coherent detection not used due to phase
Fog	0.22-272dB/km power loss	Mie scattering Photon absorption	<ul style="list-style-type: none"> • Increase transmit optical power • Hybrid FSO/RF • Diversity • More efficient modulations
Rain and Snow	20-60dB/km power loss	Photon absorption	Increase transmit optical power
Pointing stability and swaying buildings		Loss of signals. Multipath induced distortions. Low power due to beam divergence and spreading. Short term loss of signals	<ul style="list-style-type: none"> • Spatial diversity • Mesh architectures: using diverse routes

2.7 Summary

From the above discussion, it has been inferred that the main limitation of a FSO channel is caused by the atmospheric incident like turbulence, fog, rain, snow, etc. One of the solution of these problems is to increase the transmit optical power but there is a limit to the transmit power of an optical transmitter due to the eye and skin safety from laser

radiation. Another solution is to use robust and power efficient modulation technique which can reduce the channel impairments caused by atmospheric turbulence.

CHAPTER 3

MODULATION AND DETECTION TECHNIQUES

3.1 Overview

Most practical Optical Wireless Communication (OWC) systems being currently deployed employ the IM/DD scheme for outdoor as well as indoor applications [1,28]. Atmospheric conditions, in particular heavy fog, are the major problem, as the intensity of light propagating through a thick fog is reduced considerably. Therefore, intuitively, it appears that the best solution to high attenuation would be to pump more optical power or concentrate and focus more power into smaller areas. However, the eye safety introduces a limitation on the amount of optical power being transmitted. For indoor applications, the eye safety limit on transmit optical power is even more stringent. The optical channel differs significantly from the RF channels. Unlike RF systems where the amplitude, frequency and phase of the carrier signal are modulated, in optical systems, it is the intensity of the optical carrier that is modulated in most systems operating below 2.5 Gbps data rates in IM/DD. In this chapter, we will discuss about various modulation schemes and detection schemes that are commonly used in FSO systems.

3.2 Types of Modulation Schemes

In IM-DD optical wireless systems, the modulation schemes can be grouped into two general categories: base band intensity modulation and sub-carrier intensity modulation. In baseband modulation, at the optical transmitter end, the information signal directly modulates the LD drive current of optical carrier. At the receiver end, the information is

recovered using the technique of direct detection, in which the photo detector generates an electric signal according to the instantaneous power of the received optical signal. In case of sub-carrier modulation, the information signal first modulates the RF electrical subcarrier. The modulation schemes can be BPSK, QAM, FM, AM, etc. [26]. The modulated electrical sub-carrier signal in turn intensity modulates the optical carrier. At the receiver end, the signal is once again recovered by direct detection. All these techniques are non-coherent which are adopted due to low cost and low complexity of the receiver structure used in terrestrial and indoor systems. However, some of the space laser communication links do use coherent detection technique as well as with better performance, but with added complexity in the transceiver structure.

A number of digital, analog and pulse modulation techniques can be used in optical wireless schemes. Among the analog schemes AM, FM and PM can be used [1] for indoor applications. In pulse modulation, sequence of carrier pulses with a suitable parameter, such as the pulse amplitude, width or position is electrically modulated by the base band as PAM, PWM or PPM modulation respectively. Again the modulated carrier is transmitted optically by intensity modulation of the optical signal. In digital schemes, which are most commonly used because of their inherent advantage, prior to transmission the information is digitized and translated to specific code, such as RZ or NRZ codes, to get a stream of pulses which are then modulated with one of the digital schemes, i.e., OOK, PPM, DPSK, QPSK, BPSK, etc.

3.3 Selection Criterion of Modulation Scheme

Selecting the most appropriate modulation scheme will depend on some certain system criterion. For optical wireless systems, the two main criterion are:

1. Power Efficiency
2. Bandwidth Efficiency

To study the performance of any modulation format, the important parameters are bandwidth and the minimum power requirement at the receiver detector to correctly detect the signal in presence of noise. As the average optical transmitted power governs the eye safety and electrical consumption of the transmitter, it is essential to calculate the power requirement of each modulation scheme. The bandwidth requirement on the other

hand is important as it determines the maximum data rate achievable by the link with a particular modulation format.

Power efficient modulation schemes are simple to implement. The modulation schemes with short pulses, such as PPM meets the low average power requirement essential for eye safety consideration, but they require a very large bandwidth. On the other hand, at high data rate terrestrial links, bandwidth efficient schemes, like OOK, are more effective. Therefore, power efficient modulation schemes may not be always bandwidth efficient, such as PPM cannot give good performance in these schemes. On the other hand, in bandwidth efficient schemes like OOK, the restrictions on power levels due to laser eye safety regulations significantly reduce the link margin, thereby restricting the operational range. Therefore, a compromise has to be made between the power and bandwidth when selecting a modulation scheme.

3.3.1 Power Efficiency

In order to comply with the eye and skin safety regulations, the average optical power emitted by an optical wireless transceiver is limited [1,2]. Furthermore, in portable battery-powered equipment, it is desirable to keep the electrical power consumption to a minimum, which also imposes limitations on the optical transmit power. Each of the modulation schemes offers a certain optical average power, and therefore they are usually compared in terms of the average optical power required to achieve a desired BER performance or SNR. The power efficiency η_p of a modulation scheme is given by the average power required to achieve a given BER at a given data rate [3]. Mathematically, η_p is defined as [4]:

$$\eta_p = \frac{E_{pulse}}{E_b} \quad (30)$$

where E_{pulse} is the energy per pulse and E_b is the average energy per bit.

3.3.2 Bandwidth Efficiency

Although the optical carrier can be theoretically considered as having an ‘unlimited bandwidth’, the other constituents (photodetector area, channel capacity) in the system limit the amount of bandwidth that is practically available for a distortion-free communication system [2]. Also, the ensuing multipath propagation in diffuse link/nondirected LOS limits the available channel bandwidth [5]. This also makes the bandwidth efficiency a prime metric. The bandwidth efficiency η_B is defined as [4]

$$\eta_B = \frac{R_b}{B} \quad (31)$$

where R_b is the achievable bit rate and B is the bandwidth of the IR transceiver.

When the shot noise is the dominant noise source, the received SNR is proportional to the photodetector surface area. Consequently, single-element receivers favor the use of large-area photodetectors. However, the high capacitance associated with large-area photodetectors has a limiting effect on the receiver bandwidth. In addition to this, for nondirected LOS and diffuse link configurations, the channel bandwidth is limited by multipath propagation. Therefore, it follows that modulation schemes that have a high bandwidth requirement are more susceptible to intersymbol interference (ISI), and consequently incur a greater power penalty. Thus, the second most important criterion when evaluating modulation techniques is the bandwidth efficiency.

There are also other constraints, which are to be taken into consideration while selecting a modulation scheme. A modulation technique should be able to offer a minimum acceptable error rate in adverse conditions as well as show resistance to the multipath-induced ISI. In addition, the modulation technique should be resistant to a number of factors such as the phase jitter due to variations of the signal power, pulse extensions due to diffusion component larger time constant and pulse distortion due to near-field signal clipping [4,6]. Optical wireless transceivers intended for mass market applications are likely to have tight cost constraints imposed upon them. Consequently, it is highly desirable that the chosen modulation technique is rather simple to implement. Achieving excellent power efficiency and/or bandwidth efficiency is of little use if the scheme is so complex to implement that cost renders it unfeasible. Another consideration when evaluating modulation techniques is the ability to reject the interference emanating from artificial sources of ambient light. The simplest method to reduce the power level of the ambient light is to use electrical high-pass filtering. Consequently, it is desirable that the chosen modulation technique does not have a significant amount of its power located at DC and low frequencies, thereby reducing the effect of baseline wander and thus permitting the use of higher cut-on frequencies. In addition to this, if the chosen modulation technique is required to operate at medium to high data rates over non

directed LOS or diffuse links, multipath dispersion becomes an issue. Consequently, it is also desirable that the scheme be resistant to ISI resulting from multipath propagation.

3.4 Modulation Schemes used in FSO Channel

The type of modulation to be used depends on speed, distance and weather conditions. OOK is the simplest and mostly used in practical FSO system. PPM is the most power efficient but when we compare in terms of BER performance, the digital modulation schemes like BPSK, QPSK, DPSK gives better performance.

3.4.1 On-Off keying

On –Off Keying (OOK) is one of the most common modulation schemes used in practical FSO system. The transceiver structure used are most simple and the modulation schemes has high bandwidth efficiency. It is a binary level scheme with two symbols. The presence of an optical carrier wave indicates a binary ‘1’ symbol and its absence indicates a ‘zero’ symbol. Both the return-to-zero (RZ) and non return-to-zero (NRZ) schemes can be applied. In the NRZ scheme, a pulse with duration equal to the bit duration is transmitted to represent 1 while in the RZ scheme the pulse occupies only the partial duration of bit. *Figure 3-1* shows the single mapping of OOK-NRZ and OOK-RZ with a duty cycle $\lambda = 0.5$ for average transmitted power of P_{avg} . Hence, the envelop for OOK-NRZ is given by [1],

$$p(t) = \begin{cases} 2P_r, & \text{for } t \in [0, T_b] \\ 0 & \text{elsewhere} \end{cases} \quad (32)$$

Where P_r is the average power and T_b is the bit duration.

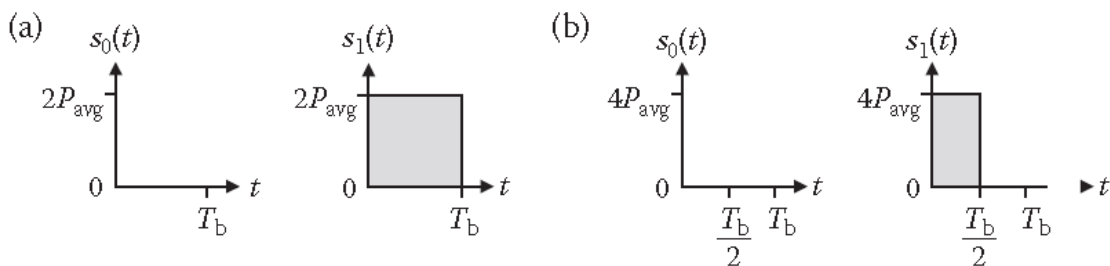


Figure 3-3: Transmitted waveforms for OOK: (a) NRZ and (b) RZ ($\lambda = 0.5$)

The OOK-NRZ has power efficiency η_p of 2 and bandwidth efficiency η_b of 1. The OOK-RZ has the same power efficiency as OOK-NRZ; however, bandwidth efficiency depends on the duty cycle. The bandwidth efficiency for $\lambda = 1/4$ is 0.25. Furthermore, RZ does not support sample clock recovery at the receiver because it allows a long low signal without any 0 to 1 transition. Therefore, bit stuffing is necessary which further decreases bandwidth efficiency.

The conditional bit error rate (P_{e-OOK}) for NRZ coded optical data with no turbulence taken into consideration, can be expressed as a function of SNR as follows[26]:

$$P_{b_{OOK}} = \frac{1}{2} \operatorname{erfc} \left(\frac{1}{2\sqrt{2}} \sqrt{SNR} \right) \quad (33)$$

3.4.2 Pulse Position Modulation

In LOS OWC links where the requirement for the bandwidth is not of a major concern, PPM with its significantly better power efficiency seems to be the most attractive option for a range of applications. PPM is an orthogonal modulation technique and a member of the pulse modulation family. The PPM modulation technique improves on the power efficiency of OOK but at the expense of an increased bandwidth requirement and greater complexity. *Figure 3-2* shows the time waveforms for PPM. An L-PPM symbol consists of a pulse of constant power occupying one slot duration within L ($= 2^M$, where bit resolution $M > 0$ is an integer) possible time slots with the remaining slots being empty. Information is encoded within the position of the pulse and the position of the pulse corresponds to the decimal value of the M -bit input data. In order to achieve the same throughput as OOK, PPM slot duration T_{s_PPM} is shorter than the OOK bit duration T_b by a factor L/M , that is–

$$T_{s_PPM} = \frac{T_b M}{L} \quad (34)$$

The transmit pulse shape for L-PPM is given by[22]-

$$x(t)_{PPM} = \begin{cases} 1, & \text{for } t \in [(m-1)T_{s_PPM}, mT_{s_PPM}] \\ 0, & \text{elsewhere} \end{cases} \quad (35)$$

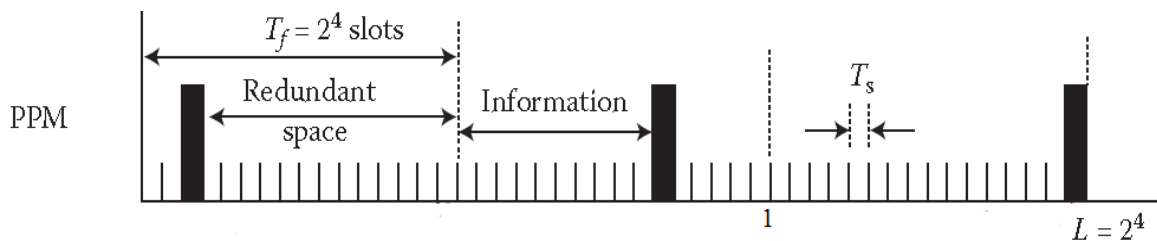


Figure 3-2: Time waveforms for PPM

In this modulation scheme, each pulse of a laser can be used to represent one or more bits of information by its position in time relative to the start of a symbol whose duration is identical to that of information bits. It contains Bits in block encoding are transmitted in blocks instead of one at a time. To achieve optical block encoding, each word of M bits is converted into one of $L=2^M$ optical fields for transmission. Since L is the possible pulse positions code for K_1 bits of information in PPM scheme, and the bit rate is expressed as follows [21]:

$$R_b = B \frac{\log_2 L}{L} \quad (36)$$

For Gaussian noise, the BER for L-PPM scheme can be expressed as:

$$P_{b_{PPM}} = \frac{1}{2} \operatorname{erfc} \zeta \quad (37)$$

With the increase of L the bandwidth requirement increases as well as the required power for transmitting the same signal.

3.4.3 Digital Phase Modulation Techniques

Phase modulation (PM) is a technique where data is sent using an alternating carrier wave and by varying the instantaneous phase of the wave. This modulation scheme can be used with both analog and digital data.

In analog PM, the phase of the carrier signal continuously varies. As a result, we get infinite number of possible phase states of the carrier wave. When the instantaneous input wave has positive polarity, the carrier phase changes in one direction and when the input waveform has negative polarity, the carrier phase shifts in the opposite direction. At any

instant of time, the amount of carrier-phase shift is directly proportional to the extent to which the amplitude of the signal is negative or positive.

In digital PM, the phase of the carrier signal changes instantaneously, rather than continuously back and forth. For the case when the number of possible phase states is two, the mode is called bi-phase modulation. There can be four, eight, or even more different phase states in more complex modes. A specific digital input data state is represented by each phase angle.

3.4.3.1 BPSK

In phase modulation technique, the information is expressed in terms of the carrier. When binary digital signal is to control the phase of a sinusoidal carrier that is called Binary Phase Shift Keying (BPSK). It is a two stage phase shift keying where the phase of the carrier is set to 0 or π , according the value of the modulating signal. If a symbol '1' is transmitted, the modulated signal is exactly as the carrier with phase 0, similarly, phase π standing for 0. The BPSK modulation is the simplest form of PSK and it more robust to resist noise than OOK.

As for BPSK, $B=R_b$, each bit of the modulating signal causes a transmitting symbol with T_s duration that equal with the bit duration T_b . That is, the required bandwidth for BPSK is equal to the bit rate. This is consistent with the OOK. According to the definition of bandwidth efficiency, the bandwidth efficiency for BPSK can be expressed as follows[22]:

$$\eta_{BPSK} = \frac{R_b}{B} = 1 \quad (38)$$

This the theoretical bandwidth efficiency for BPSK is unit. And the conditional BER of BPSK is[23]:

$$P_{b_{BPSK}} = \frac{1}{2} \text{erfc}(\sqrt{SNR}) \quad (39)$$

The power requirements can readily be derived from the BER expressions.. In the case of equal BER, using the normalized average power requirements of BPSK to NRZ-OOK, the power requirement for BPSK can be written as:

$$\frac{P_{BPSK}}{P_{OOK}} = \frac{1}{2\sqrt{2}} \quad (40)$$

Theoretically, the NRZ-OOK requires as much as $2\sqrt{2}$ times power than BPSK to achieve particular BER performance.

3.4.3.2 DPSK

DPSK is a relative phase modulation model, the information which is transmitted equals 0, this $\Delta\phi$ represented by the phase difference between the adjacent symbols. Which means two adjacent symbol signals that before and after are the same. Therefore, the phenomenon of inverted π can be avoided with DPSK modulation scheme. As synchronous demodulation, compared to BPSK modulation, there is no need to know the phase and frequency of the carrier, but the local carrier is necessary. The BER for DPSK can be calculated as follows[22]:

$$P_{b_{DPSK}} = \frac{1}{2} \operatorname{erfc}\left(\frac{\sqrt{(SNR)}}{\sqrt{2}}\right) \quad (41)$$

When using differential decoding, the information bit “1” will be transmitted by shift the phase of modulated signal 180° relative to the previous phase of the modulate signal. And bit '0' will be transmitted without shift the phase of modulated signal relative to the previous of modulated signal. The required bandwidth for DPSK is equal to the bit rate, $B_{DPSK}=R_b$.

The spectrum efficiency of DPSK is relatively higher, dispersion tolerance, nonlinear tolerance and PMD tolerance can be improved. When getting the same bit error rate, the receiver sensitivity is 3dB higher than OOK modulation. In terms of resisting noise, it is better than OOK. The bandwidth efficiency is equal to BPSK and OOK, that is:

$$\eta_{DPSK}=1 \quad (42)$$

The average power requirement of DPSK normalized to OOK can be expressed as

$\frac{P_{DPSK}}{P_{OOK}} = \frac{1}{2\sqrt{2}}$. Under the same BER condition, the average power of NRZ-OOK is twice than DPSK[24].

3.4.3.3 QPSK

Different from BPSK and DPSK, the QPSK scheme uses two bits are grouped together to form signals. When signals transmitted, there are four particular phases. The spectral efficiency can be further enhanced by QPSK modulation. Since the QPSK can be regarded as the composition of two orthogonal signals of BPSK. Therefore, each bit occupies T_b seconds, the signals corresponding to the bits last for $T_s=2T_b$.

This means that the required bandwidth for QPSK is double to BPSK modulation, that is, $B_{QPSK}=0.5R_b$. And the theoretical bandwidth efficiency for QPSK is:

$$\eta_{QPSK} = \frac{R_b}{0.5 R_b} \quad (43)$$

But, the practically the bandwidth efficiency is $1.4 \sim 1.6$ bps/Hz. Since the QPSK is a four-state phase shifting keying in which two bits are grouped together and the carrier is phase modulated, each bit has half of the original received intensity. Therefore, BER for QPSK can be considered as two orthogonal of BPSK combined. BER for QPSK can be described as[24]:

$$P_{b_{QPSK}} = \text{erfc}(\sqrt{SNR}) = 2 P_{b_{PSK}} \quad (44)$$

Consequently, the average power requirement by QPSK normalized to NRZ-OOK can be expressed as:

$$\frac{P_{QPSK}}{P_{OOK}} = \frac{1}{2\sqrt{2}} \frac{\text{erfc}^{-1}(BER)}{\text{erfc}^{-1}(2BER)} \quad (45)$$

Therefore the average power requirement of QPSK is almost equal to BPSK, only a few amount of power more than BPSK is required. QPSK is bandwidth efficient than anyother modulation schemes[25].

3.4.4 QAM

The creation of symbols that are some combinations of amplitude and phase can carry the concept of transmitting more bits per symbol further. This method is called quadrature amplitude modulation (QAM). For example, 8QAM uses four carrier phases plus two amplitude levels to transmit 3 bits per symbol[18]. Other popular variations are 16QAM, 64QAM, and 256QAM, which transmit 4, 6, and 8 bits per symbol respectively. *Figure 3-3* represents the constellation diagram of a 16-QAM.

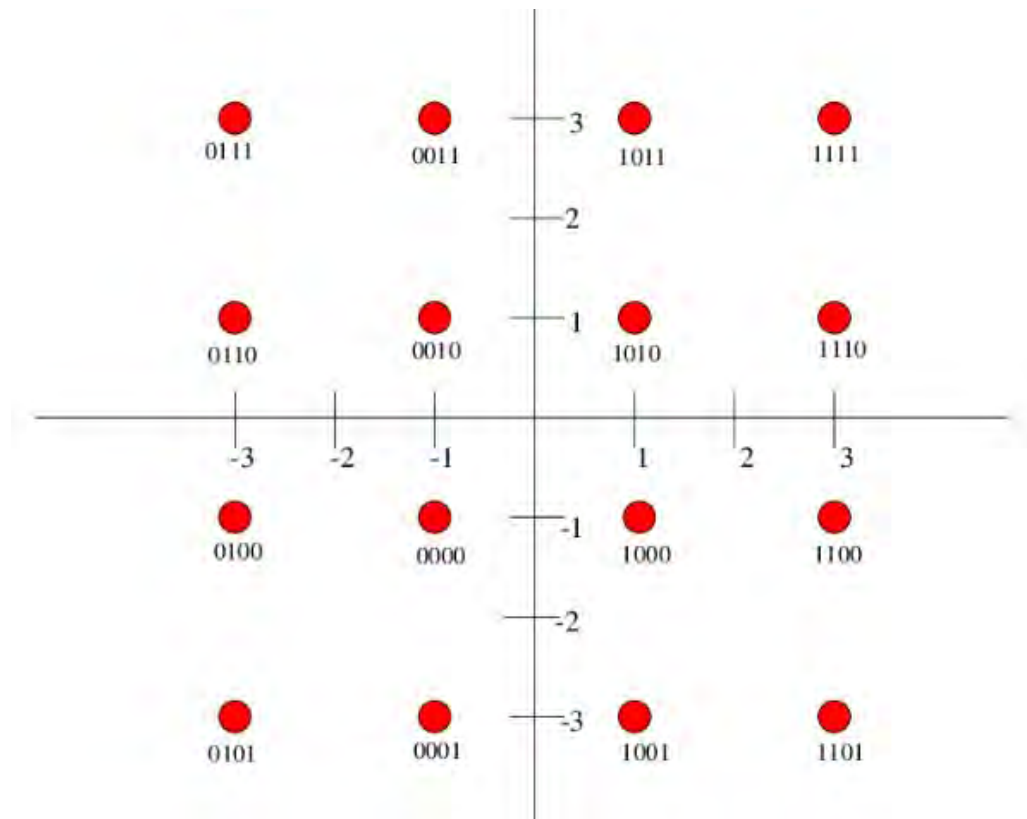


Figure 3-3:16-QAM constellation diagram

While QAM is enormously efficient of spectrum, it is more difficult to demodulate in the presence of noise, which is mostly random amplitude variations. Linear power amplification is also required. QAM is very widely used in cable TV, WiFi wireless local area networks (LANs), satellites, and cellular telephone systems to produce maximum data rate in limited bandwidths.

3.4.5 OFDM FSO System

OFDM is a popular modulation/multiplexing technique for broadband wireless communication which is robust to multipath fading and frequency selective fading [6]. By this virtue, OFDM has become a modulation technique for IEEE 802.11a Wireless Local Area Network and IEEE 802.16 standards. Combining OFDM with FSO gives rise to OFDM based FSO, which will exploit the advantages of both, becomes a good candidate for “last mile” solution for broad band connectivity with high speed data rates [1,7].

OFDM-FSO system support high data rates by splitting a high-rate data-stream into a number of low-rate data-streams and transmitting these over a number of narrowband

subcarriers. The narrowband subcarrier data-streams experience smaller distortions than high-speed ones and require no equalization. Moreover, most of the required signal processing is performed in the free space domain. This is advantageous because microwave devices are much more mature than their optical counterparts and because the frequency selectivity of microwave filters and the frequency stability of microwave oscillators are significantly better than that of corresponding optical devices. The subcarriers are themselves modulated by using phase shift keying (PSK) or quadrature amplitude modulation (QAM) and are then carried on a high frequency carrier [1]. The OFDM signal for N subcarriers, after up-conversion to the wireless service carrier frequency f_c , can be written as:

$$S_{OFDM}(t) = \sum_{n=0}^{N-1} S_n(t) \quad (46)$$

The first raw data is mapped according to different types of modulation techniques (BPSK, QPSK, 8-PSK, 16-QAM, 64-QAM), depending upon data rate. Representing the equation (46) in complex data symbol,

$$S_{OFDM}(t) = \sum_{n=0}^{N-1} X_n(\exp(j(\omega_n + 2\pi f_c t))) \quad (47)$$

The above equation represents each symbol X_n is amplitude modulated on orthogonal subcarriers. This process is performed using the IFFT which guarantees that all the subcarriers are orthogonal to each other over the symbol interval. Here, we set the guard interval to zero and thus the OFDM symbol duration T_s equals to the Fourier analysis window. The $S_{OFDM}(t)$ is real by enforcing the conjugate-symmetry (Hermitian symmetry) of the IFFT input vector, The first input X_0 , corresponding to the zero frequency, needs to be real-valued and is generally left unmodulated. This approach with real-valued IFFT output is used in digital subscriber line (DSL) systems and is known as Discrete Multitone (DMT). Due to frequency selectivity, the subcarriers experience in general different channel gains, which can be mitigated through the use of many narrow subcarriers. The signal $S_{OFDM}(t)$ is then used to modulate the optical intensity of laser diode (LD) to be transmitted through fiber optics [1].

OFDM can be simply defined as a form of multicarrier modulation, where its carrier spacing is carefully selected so that each subcarrier is orthogonal to the other subcarriers and can be separated at the receiver by correlation techniques, hence, inter symbol interference among channels can be eliminated. The set of orthogonal carriers is realized

by using the inverse fast Fourier transform (IFFT) at the transmitter. In addition, the channel estimation based on block type pilot arrangement is performed by sending pilots at every sub-channel and using this estimation for a specific number of following symbols [8]. The input signal is taken as series of bits/symbols, which are base band modulated, also called mapping. This converts the signal into complex form. The mapped signal is converted from serial to parallel form and IFFT is computed to obtain the OFDM symbol. To the generated OFDM symbol, cyclic prefix (CP) bits/guard bands are added for improved system performance followed by parallel to serial conversion and digital to analog conversion. At the receiver, the reverse process is carried out after being detected by the photodiode and FFT is taken to convert the OFDM symbol back into complex bit sequences. Thus, de-mapping converts the complex signal into original bit sequences.

3.5 Detection Techniques in a FSO System

Photodetection is the process of converting information-bearing optical radiation into its equivalent electrical signal with the aim of recovering the transmitted information. At the transmitter, the information can be encoded on the frequency, phase or the intensity of the radiation from an optical source. This encoded radiation is then transmitted to the receiver via the free-space channel or the optical fiber. The receiver front-end devices (telescope and optical filter) focus the filtered radiation onto the photodetecting surface in the focal plane. There are two possible detection schemes widely adopted in optical communications: IM-DD and coherent schemes. IM-DD is the simplest and widely used. Coherent detection schemes offer the potential of restoring full information on optical carriers, namely the amplitude (in-phase (I) component) and phase (quadrature (Q) component) of the complex optical electric field and the state of polarization of the signal [15]. However, such receivers are sensitive to the phase and the state of polarization of the received optical signal.

3.5.1 Direct Detection

In intensity-modulation direct detection, only one degree of freedom, the intensity of the light emitted from an LD or an LED, is employed to convey the information. In direct detection scheme, a local oscillator is not used in the detection process and for this type of receiver to recover the encoded information, it is essential that the transmitted

information be associated with the intensity variation of the transmitted field. *Figure 3-4* shows a block diagram of a FSO system using IM/OOK and APD receiver.

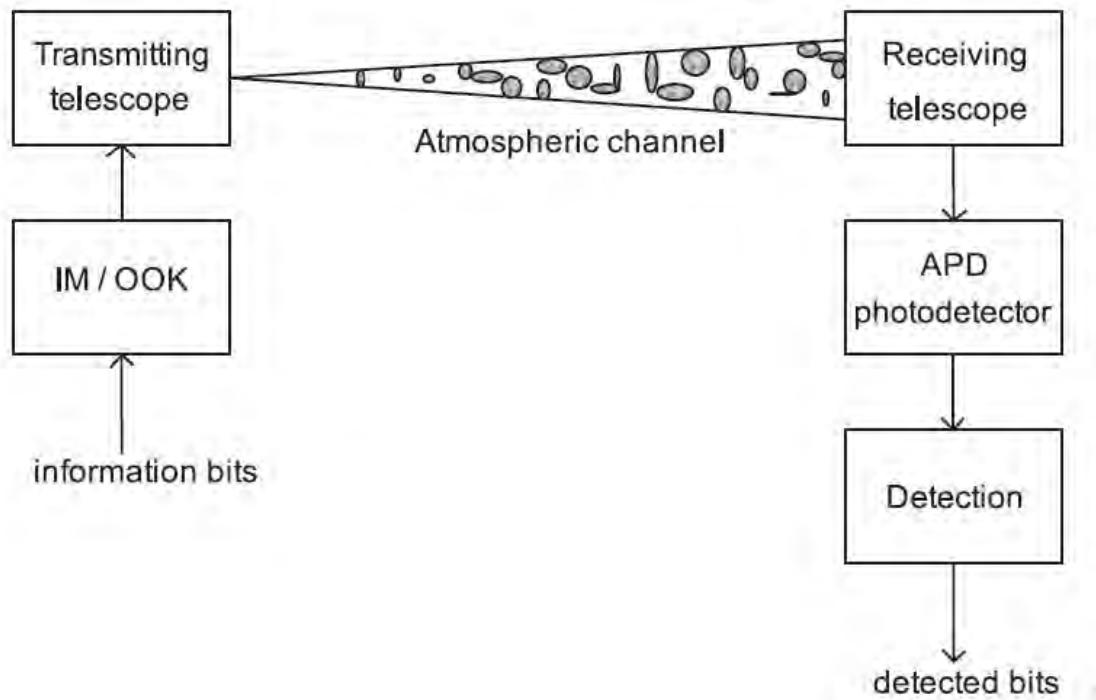


Figure 3-4 : Block diagram of a FSO system using IM/OOK and APD receiver

Hence, this type of detection is also known as the envelope detection. For an instantaneous incident power $P(t)$, the instantaneous photodetector current $i(t)$ is given by-

$$i(t) = \frac{\eta_{qe} \lambda q}{hc} MP(t) \quad (47)$$

where M is the photodetector gain factor whose value is unity for the PIN photodetector.

The block diagram of the direct detection receiver is illustrated in *Figure 3-5* below:

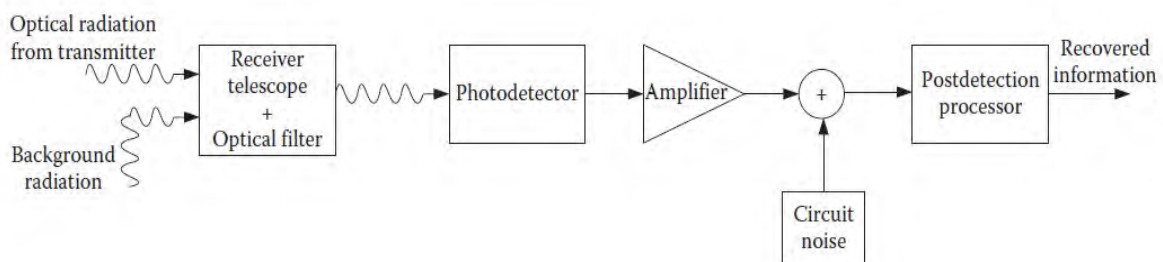


Figure 3-5: Block diagram of a direct detection Receiver

3.5.2 Coherent Detection

In coherent optical communications, the optical signal is modulated by the information using amplitude, phase and frequency of the lightwave. At the receiving end, an optical local oscillator (OLO) is used and by combining the OLO with the received signal, optical heterodyne or homodyne detection is performed [16]. The frequency of the local oscillator does not have to be the same as that of the incoming information-bearing radiation. This possibility is thus responsible for the two variants of coherent detection discussed below. In coherent heterodyne detection schemes, the OLO frequency is about several gigahertz different from the optical frequency of the received optical signal. The basic block diagram of a coherent receiver is shown in *Figure 3-6* below:

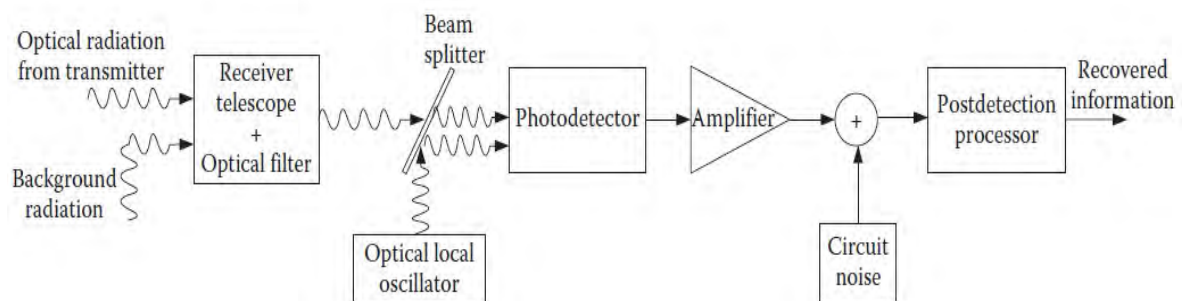


Figure 3-6: Block diagram a coherent detection scheme

It is pertinent to clarify that the term ‘coherent detection in optical detection’ is not synonymous with coherent detection in RF parlance. In contrast to RF coherent detection, the output of the local oscillator in optical coherent detection is not required to have the same phase as the incoming radiation. The electric fields of the received optical and the local oscillator signals are defined as-

$$E_c(t) = A_c \exp [-i(\omega_c t + \theta_c)] \quad (48)$$

$$E_L(t) = A_L \exp [-i(\omega_L t + \theta_L)] \quad (49)$$

where A_c and θ_c are the amplitude and phase of the carrier field, respectively, while the local oscillator amplitude and phase are A_L and θ_L in that order. The generated

photocurrent at the output of the photodetector, which operates as a square-law device, is given by-

$$i_{IF-C}(t) = RM(E_C + E_L)^2 \quad (50)$$

Since the optical power is proportional to the intensity, the received optical power is defined by-

$$P(t) = P_C + P_L + 2\sqrt{P_C P_L} \cos(\omega_{IF} + \theta_C - \theta_L) \quad (51)$$

Where, $P_C = kA_C^2$

$$P_L = kA_L^2$$

$$\omega_{IF} = \omega_0 - \omega_L$$

Depending on whether the intermediate frequency ω_{IF} is equal to zero or not, there are two different coherent detection schemes known as heterodyne and homodyne, as outlined below.

3.5.2.1 Heterodyne Detection

In a heterodyne detection optical receiver, the incoming radiation (carrier) is combined with a reference wave from the OLO (i.e., a laser) on the photodetector surface as shown in *Figure 3-6*. This optical mixing process produces another wave at the intermediate frequency ω_{IF} by the square-law characteristics of the photodetector [1]. This ω_{IF} , which is the difference between the incoming laser carrier and the reference OLO signal frequencies, passes through a band-pass filter to an electrical second detector (the postdetection processor in *Figure 3-6*) for the final demodulation. When the instantaneous field amplitudes $E_C(t)$ and $E_L(t)$ in Equations (13) and (14) combine on the photodetector surface, they produce an instantaneous signal whose intensity is given by –

$$C(t) = (E_C(t) + E_L(t))^2 \quad (52)$$

The time average of $C(t)$ multiplied by the responsivity gives the resultant instantaneous carrier and local oscillator current $i_p(t)$, at the photodetector output. Hence,

$$i_p(t) = R i \quad (53)$$

The first two terms are time invariant, the third term is very slowly varying with respect to the short time over which the average is taken, while the fourth term is out of the IF band [1]. Equation (18) is now reduced to-

$$i_p(t) = R \left\{ \frac{A_L^2}{2} + \frac{A_c^2}{2} + 3rd\ term + 4th\ term \right\} \quad (54)$$

Therefore, the IF filter, which is an integral part of the postdetection processor of *Figure 3-6*, only allows the third term to go through while the others are suppressed, resulting in the following expression for the instantaneous current:

$$i_p(t) = R A_L A_c \cos \dot{\phi} \quad (55)$$

The above result makes it possible to recover any information impressed on the carrier field amplitude, frequency or even phase. The following points can therefore be deduced from this that heterodyne detection offers:

1. A relatively easy means of amplifying the photocurrent by simply increasing the local oscillator power.
2. Improved SNR is achieved by increasing the local oscillator power so much that its inherent shot noise dwarfs the thermal and the shot noise from other sources.

However, the frequency of an optical source is known to drift over time. Therefore, the ω_{IF} needs to be continually monitored at the input of the electrical detector and the local oscillator frequency varied accordingly to keep the IF centre frequency constant. Also, the optical source, particularly a laser, does suffer from phase noise which means that θ_c and θ_L in Equation (20) are not absolutely fixed; they fluctuate. These factors contribute to the challenges of implementing a coherent optical communication system.

3.5.2.2 Homodyne Detection

This is similar to the heterodyne detection process discussed above except that the OLO has the same frequency and phase as the incoming optical radiation/carrier, so that the modulated light signal can be directly demodulated at the photodetector into the baseband signal for further processing [21]. The resultant photocurrent thus contains the information signal at the baseband. Following the same step as in heterodyne detection, the instantaneous photocurrent is obtained below-

$$i_p(t) = R \left\{ \frac{A_L^2}{2} + \frac{A_c^2}{2} + \langle A_L A_c \cos(\theta_L - \theta_c) \rangle + \langle A_L A_c \cos(2 \cos \omega_{c_0} t + \theta_L + \theta_c) \rangle \right\} \quad (56)$$

The third term is time invariant and the fourth term is suppressible via filtering to obtain

$$i_p(t) = R \left\{ \frac{A_L^2}{2} + \frac{A_c^2}{2} + A_L A_c \cos(\theta_L - \theta_c) \right\} \quad (57)$$

By increasing the locally generated radiation power such that $A_c A_L \gg 0.5 A_c$ [21], expression (22) reduces to-

$$i_p(t) = R \left[A_L A_c \cos(\theta_L - \theta_c) \right] \quad (58)$$

In coherent detection systems, the noise in the receiver is mainly dominated by OLO-induced shot noise [22]. The shot noise-limited receivers offer improved sensitivity, by up to 20 dB, compared to the IM-DD schemes [23]. In IM-DD systems, the optical carrier signals must be aligned at a large spacing in the optical wavelength domain. This is because of the bandwidth of the optical band-pass filter (OBPF), which is 2–3 nm. Therefore, the spacing between the optical carriers should be no less than several nanometers, which corresponds to hundreds to thousands of gigahertz. By using coherent schemes, the optical carrier signal could be aligned closely at a spacing 10 times or more than the data rate in the frequency domain; thus the possibility of employing frequency division multiplexing

3.6 Summary

In this section, different modulation and detection techniques for free space optical system have been discussed. The OOK is the simplest modulation scheme but it has higher BER. PPM is the power efficient scheme but it is more susceptible to slot synchronization error. Among the digital modulation schemes, QPSK is the most bandwidth efficient scheme but BPSK has better BER performance than QPSK. Direct detection is simpler than Coherent detection but there is an optical local oscillator, which contributes to higher received optical power of the photodetector.

CHAPTER 4

PROPOSED COHERENT FSO SYSTEM AND PERFORMANCE ANALYSIS

4.1 Overview

In this chapter, the proposed coherent FSO system is discussed in detail. The block diagram and analytical model is presented in this chapter. The system is simulated in MATLAB to analyze the performance of the FSO system for different modulation techniques.

4.2 Description of the proposed coherent FSO system

The proposed coherent FSO system consists of a laser source, a transmitter, a receiver and a continuous wave local oscillator beam before it strikes the photo-detector.

4.2.1 Analytical Model

The output signal of the modulator is transmitted via atmospheric channel. The overall architecture of coherent system is shown in *Figure 4-1*.

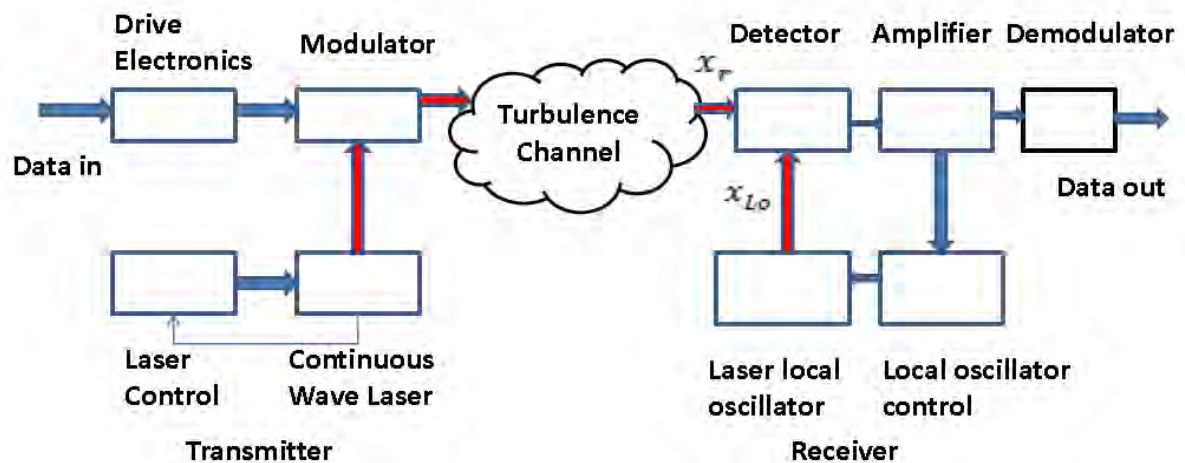


Figure 4-4: Block diagram of the coherent FSO system

The transmitting module consists of a pulse generator, a modulator, a spectrum analyzer and a transmitter. The pulse generator used in the link generates pulses that carry information in electrical form. Spectrum analyzer is used to display the scale of an input signal versus frequency within the complete frequency range of the device. Then, the signal is transmitted over free space through the transmitter. In the atmosphere, the signal is scattered, absorbed and attenuated as a result of turbulences and atmospheric variations.

The receiver on the other end includes an amplifier, photo detector, filter and Optical Local Oscillator (OLO) for properly retrieving the information signal. The amplifier used in the link improves the signal strength of received signal. The photo detector detects the incoming optical signal and after converting it to electrical form transmits the signal to filter. The filter reduces the environment noise and enables the passage of the desired wavelength of the signal through it.

The electric field of the received optical and the local oscillator's signals are [5]:

$$x_r(t) = E_r I e^{(2\pi f_c t + \frac{\alpha t}{2})} \quad (59)$$

$$x_{Lo}(t) = E_{Lo} e^{2\pi f_c t} \quad (60)$$

where, E_r and E_{Lo} are the electric field of the received signal and the local oscillator laser respectively, I is the intensity fading coefficient, $\alpha = \pm 1$ is the information, f_c is the optical carrier frequency. The total power of the received signal and local oscillator laser is:

$$\begin{aligned} P_T &= |IE_r + E_{Lo}|^2 \\ &= I^2 E_r^2 + E_{Lo}^2 + 2IE_r E_{Lo} \\ &= I^2 P_r + P_{Lo} + 2I\sqrt{(P_r P_{Lo})} \cos(\dots) \end{aligned} \quad (61)$$

where P_s and P_{Lo} are the power of the received signal and local oscillator respectively. Additionally, the output current of the photo-detector is:

$$i_p(t) = RP_T + i_{sh}(t) + i_{th}(t) \quad (62)$$

where R is the responsivity of the receiver, $i_{sh}(t)$ is the shot noise and $i_{th}(t)$ is the thermal noise. PIN photodetector is used in the analysis. Here, shot noise of the receiver is ignored and only the local oscillators shot noise is taken into consideration due to sufficiently large local oscillator power. The shot noise and thermal noise can be modeled as the stationary Gaussian random process with the zero-mean value and variance.

The shot noise power of the local oscillator [1]:

$$\sigma_{sh}^2 = 2eB \langle i_{Lo} \rangle \quad (63)$$

And the thermal noise power at the local oscillator [1]:

$$\sigma_{th}^2 = \frac{4kTB}{R_L} \quad (64)$$

The total noise power at the output is given by [10]:

$$\begin{aligned} \sigma_n^2 &= \sigma_{sh}^2 + \sigma_{th}^2 \\ &= 2eB \langle i_{Lo} \rangle + \frac{4kTB}{R_L} \\ &= 2eBR P_{Lo} + \frac{4kTB}{R_L} \quad (65) \end{aligned}$$

where R_L is the load resistance.

The instantaneous SNR is given by:

$$\begin{aligned} SNR(I) &= \frac{\text{Signal Power}}{\text{Noise Power (Thermal noise + Shot noise)}} \\ &= \frac{(2IR E_r E_{Lo})^2}{2eBR P_{Lo} + \frac{4kTB}{R_L}} \\ &= \frac{(2IR)^2 \times P_r P_{Lo}}{2eBR P_{Lo} + \frac{4kTB}{R_L}} \quad (66) \end{aligned}$$

As the Local oscillator power is large, the second part of the denominator can be ignored.

4.2.2 Channel Model

The Gamma-Gamma turbulence model has been widely used to study the turbulent behaviour of the atmosphere. This model is suitable for both weak and strong turbulence regime. The beam intensity fluctuation probability density of Gamma-Gamma model is given by [8]:

$$f(I) = \frac{2(\alpha\beta)^{\frac{\alpha+\beta}{2}}}{\Gamma(\alpha)\Gamma(\beta)} I^{\left(\frac{\alpha+\beta}{2}-1\right)} K_{\alpha-\beta}(2\sqrt{\alpha\beta I}) \quad (67)$$

where, $I > 0$ is the received signal irradiance, α and β are the parameters of probability density function, Γ is the Gamma function and K_a is the modified Bessel function of second kind of order a . Here, α and β are the effective number of small scale and large scale eddies of turbulent environment, which are given by [45]:

$$\alpha = \left\{ \exp \left[\frac{0.49 \sigma_R^2}{\left(1 + 1.1 \sigma_R^{\frac{12}{5}}\right)^{\frac{7}{6}}} \right] - 1 \right\}^{-1} \quad (68)$$

$$\beta = \left\{ \exp \left[\frac{0.49 \sigma_R^2}{\left(1 + 1.1 \sigma_R^{\frac{12}{5}}\right)^{\frac{7}{6}}} \right] - 1 \right\}^{-1} \quad (69)$$

$$\sigma_R^2 = 1.23 C_n^2 k^{7/6} L^{11/6} \quad (70)$$

where, $\sigma_R^2 = 1.23 C_n^2 k^{7/6} L^{11/6}$ is called the Rytov variance which represents the variance of log-intensity fluctuation. C_n^2 is the refractive-index structure parameter and its value ranges from 10^{-13} to 10^{-17} , k is the wave number and L is the distance between transmitter and receiver. When $\sigma_R^2 < 1$, it means the light intensity fluctuation is weak and $\sigma_R^2 > 1$ means strong intensity fluctuation.

4.2.3 Modulation Techniques Used in the Analysis

In recent times, one of the main goal of modulation is to squeeze as much data into the least amount of possible spectrums. Moreover, advanced data modulation technique can compensate the impairments caused by atmospheric turbulence. Selecting the more appropriate modulation scheme will depend on certain system requirement criterion. For optical wireless systems, the two main criterions are: power and bandwidth efficiency.

Since the average optical power emitted by an optical transmitter is always limited, the performance of modulation techniques is often compared in terms of BER at a given data

rate. Different kinds of modulation schemes are suitable for FSO communication systems. In this analysis, we have used OOK, BPSK, DPSK and QPSK modulation schemes.

The average BER of the coherent system, considering the atmospheric turbulence channel:

$$P'_b = \int_0^{\infty} P_b(I) f(I) dI \quad (71)$$

here, $f(I)$ is the PDF of Gamma-Gamma distribution. For different modulation technique $P_b(I)$, the conditional BER would be different.

The conditional BER expressions for different modulation schemes is as follows:

$$P_{b_{OOK}} = \frac{1}{2} \operatorname{erfc} \left(\frac{1}{2\sqrt{2}} \sqrt{SNR} \right) \quad (72)$$

$$P_{b_{DPSK}} = \frac{1}{2} \operatorname{erfc} \left(\frac{1}{\sqrt{2}} \sqrt{SNR} \right) \quad (73)$$

$$P_{b_{QPSK}} = \operatorname{erfc}(\sqrt{SNR}) \quad (74)$$

$$P_{b_{BPSK}} = \frac{1}{2} \operatorname{erfc}(\sqrt{SNR}) \quad (75)$$

We have calculated average BER for different modulation techniques, varying the required received power as well as SNR.

If we consider BPSK modulation technique, equation (55) becomes:

$$P'_{b_{BPSK}} = \int_0^{\infty} P_{b_{BPSK}}(I) f(I) dI \quad (76)$$

here, $f(I)$ is the PDF of Gamma-Gamma distribution.

Now inserting Equation (59) on (60), the average BER of the FSO link with BPSK modulation scheme is as follows:

$$P'_{b_{BPSK}}(I) = \int_0^{\infty} P_{b_{BPSK}}(I) f(I) dI = \frac{1}{2} \int_0^{\infty} \operatorname{erfc}(\sqrt{SNR(I)}) f(I) dI \quad (77)$$

Similarly for other modulation technique the average BER for OOK, DPSK, QPSK is as follows:

$$P_{b_{OOK}}'(I) = \int_0^{\infty} P_{b_{OOK}}(I) f(I) dI = \frac{1}{2} \int_0^{\infty} \operatorname{erfc}\left(\frac{1}{2\sqrt{2}} \sqrt{\operatorname{SNR}(I)}\right) f(I) dI \quad (78)$$

$$P_{b_{DPSK}}'(I) = \int_0^{\infty} P_{b_{DPSK}}(I) f(I) dI = \frac{1}{2} \int_0^{\infty} \operatorname{erfc}\left(\frac{\sqrt{\operatorname{SNR}(I)}}{\sqrt{2}}\right) f(I) dI \quad (79)$$

$$P_{b_{QPSK}}'(I) = \int_0^{\infty} P_{b_{QPSK}}(I) f(I) dI = \int_0^{\infty} \operatorname{erfc}\left(\sqrt{\operatorname{SNR}(I)}\right) f(I) dI \quad (80)$$

Bandwidth efficiency is another prime metric which is used to compare different modulation techniques performance. The bandwidth efficiency η_b can be defined as:

$$\eta_b = \frac{R_b}{B} \quad (81)$$

Where R_b is the achievable bit rate and B is the required bandwidth. For OOK, BPSK and DPSK schemes, bandwidth efficiency is 1 [9]. QPSK is very spectrally efficient since each carrier phase represents two bits of data. The spectral efficiency is 2 bits/Hz, meaning twice the data rate can be achieved in the same bandwidth as OOK, BPSK, DPSK. The band width efficiency of QPSK is:

$$\eta_{QPSK} = \frac{R_b}{0.5 R_b} = 2 \quad (82)$$

4.3 Results and Discussion

In this section, investigation has been carried out to evaluate the BER performance of a coherent FSO system. Simulation has been carried out using MATLAB following the derivations from previous chapter. OOK, BPSK, DPSK, QPSK modulation schemes are employed on the FSO system and analysis was done under MATLAB platform. The simulation parameters used in the analysis are given below:

Table 4-1: Simulation parameter of the proposed coherent FSO system

Parameters	Value
Receiver Bandwidth (B)	2.5 Gbps
Responsivity (R)	0.85 A/W

Temperature	300k
Load Resistance(R_L)	50 Ω
Boltzman's Constant	1.38×10^{-23} W/kHz
Refractive Index structure parameter C_n^2	10^{-14} m ^{-2/3}
Optical Wavelength(λ)	1550 nm
Electron Charge(e)	1.6×10^{-19} C
Rytov variance(σ_R^2)	0.2-6
Data rate (R_b)	2.5 Gbps

Figure 4-2 shows probability density curves for gamma-gamma model with different values of turbulence strength. The strength of the atmospheric turbulence is indicated by different values of Rytov variance (σ_R^2). The values of alpha and beta indicate whether the atmospheric turbulence region is weak, moderate or strong. When the value σ_R^2 is less than unity, it indicates weak turbulence strength. For moderate turbulence, the value of σ_R^2 is 1 and $\sigma_R^2 > 1$ indicates strong turbulence regime.

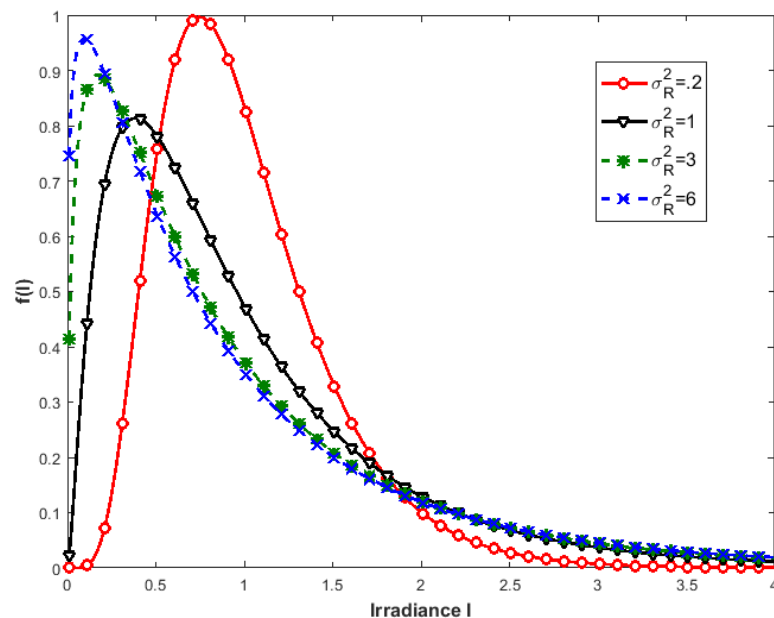


Figure 4-2: Gamma-Gamma PDF for different turbulence strength

The BER performance of the coherent FSO system is a function of the required received power level. This power is the summation of the power of the received signal in the photo detector and the local oscillator laser. For a certain value of turbulence

strength, the average required receiver power is varied. *Figure 4-3* represents the results of average BER, $P_b(I)$ as a function of average SNR for the four different modulation techniques like OOK, BPSK, DPSK, QPSK for $\sigma_R^2=0.2$. It is clearly seen that BPSK gives better BER performance. The BER values of BPSK is slightly higher than QPSK. From *Figure 4-3*, it is seen that for achieving a BER of 10^{-8} the value of SNR for OOK, DPSK, QPSK and BPSK are 27.985 dB, 21.965 dB, 19.265 dB, 18.995 dB respectively. So, the power requirement for OOK is relatively higher than other modulation schemes for getting same BER. BPSK gives best BER vs. SNR performance among the modulation techniques.

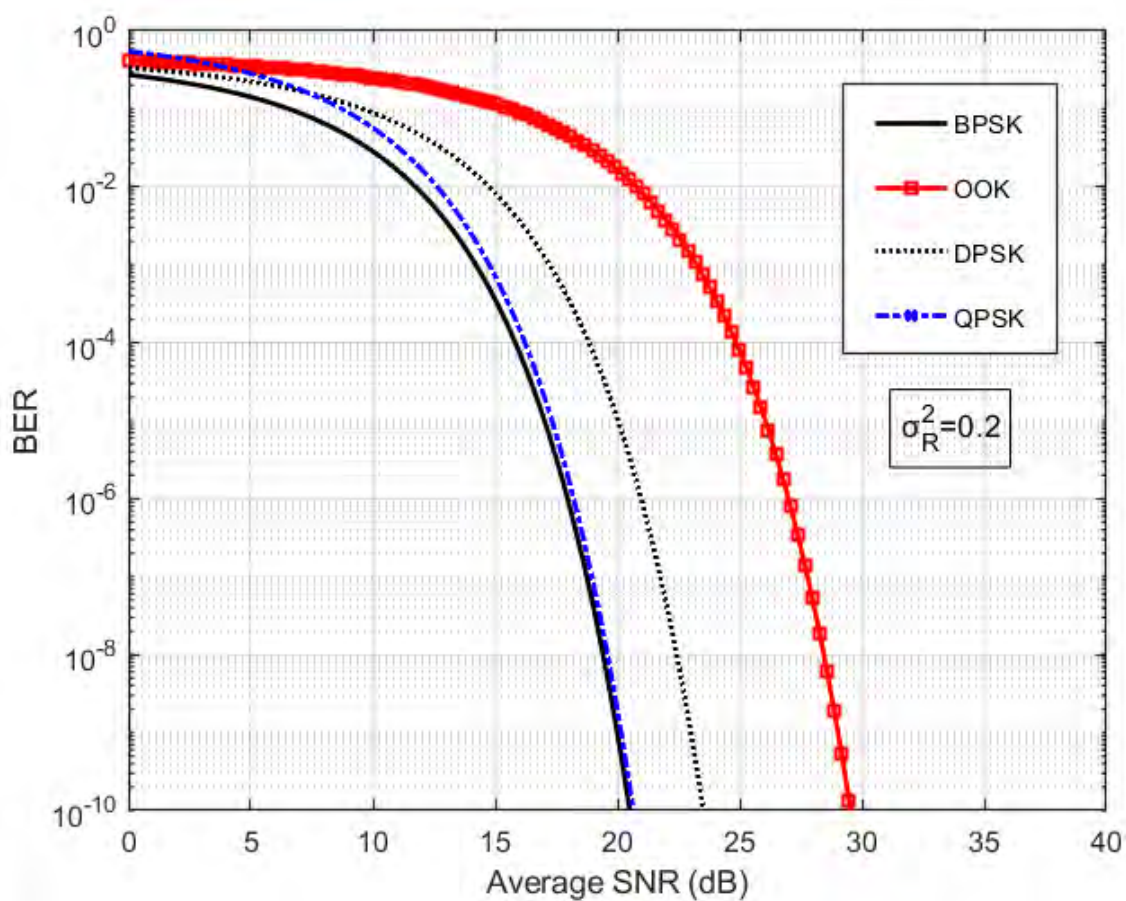


Figure 4-3: Comparison of BER performance as a function of average SNR for $\sigma_R^2=0.2$.

Figure 4-4 presents the BER vs. SNR curve of the four modulation techniques for $\sigma_R^2=1$. BPSK and QPSK give overlapping performance after 20dB SNR. As the strength of turbulence increased, the SNR value increases for getting same BER for a specific BER than $\sigma_R^2=0.2$. For BPSK, 23dB SNR needed for a BER of 10^{-10} whereas 20 dB SNR was needed in the *Figure 4-3*, where the system was simulated for a Rytov variance of value 0.2.

Figure 4-5 represents the simulated result for a Rytov variance (σ_R^2) of value 3. The turbulence is strong and more power is required than the previous two cases to attain same BER value. The BPSK gives better performance than QPSK upto 25 dB SNR and after that SNR value, these two schemes give almost equal performance. The OOK requires more power than the other three modulation schemes and its performance deteriorates than weak ($\sigma_R^2=0.2$) and moderate turbulence ($\sigma_R^2=1$) regime. Here, BPSK requires 27dB SNR to attain the BER of 10^{-8} .

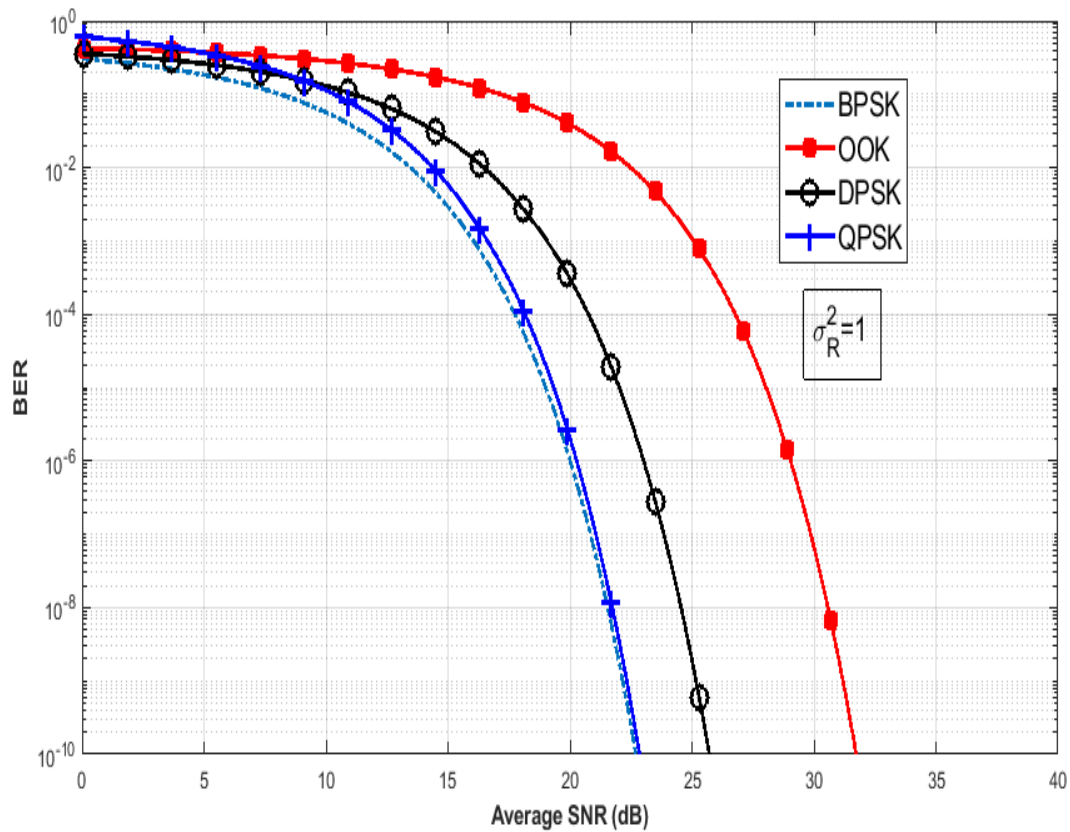


Figure 4-4: Comparison of BER performance as a function of average SNR for $\sigma_R^2=1$

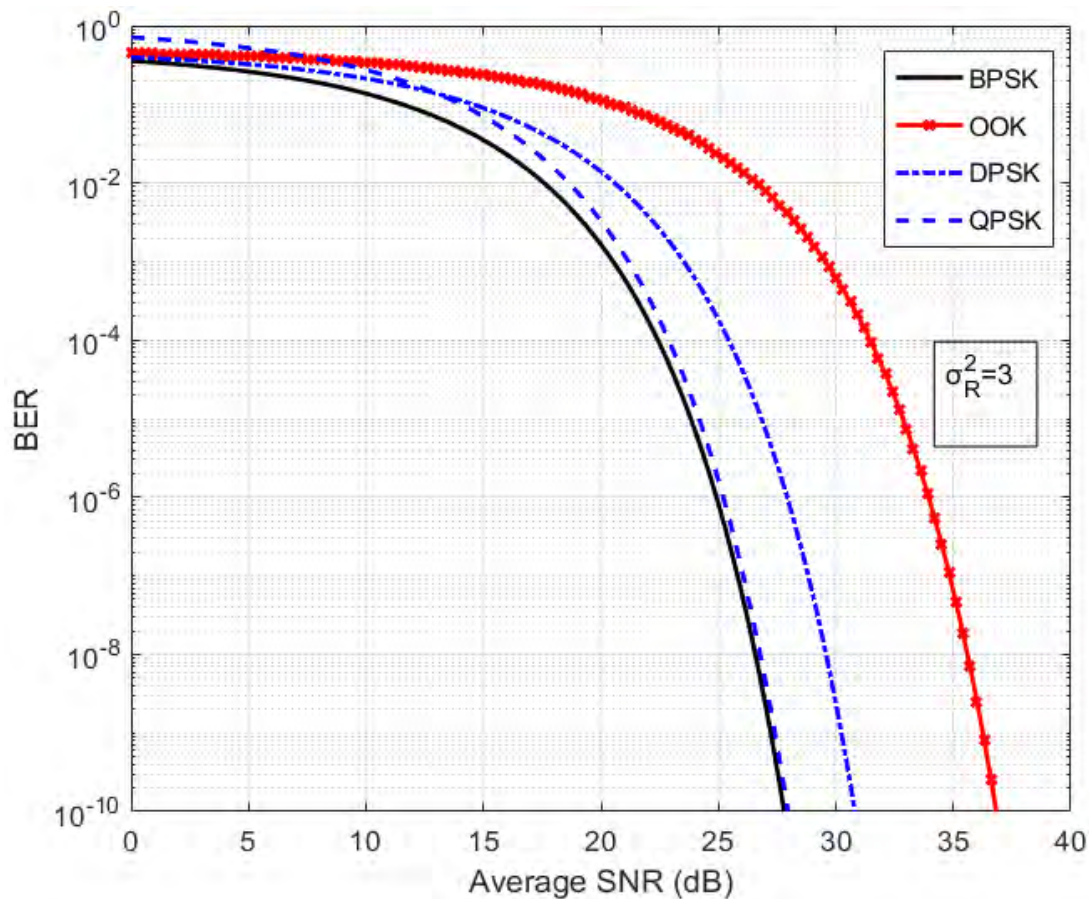


Figure 4-5: Plots of BER vs. SNR for different modulation technique for $\sigma_R^2=3$ BER vs. required received power has been plotted in *Figure 4-6* for $\sigma_R^2=1$ which is a moderate turbulence condition. The system is consistent for a BER upto 10^{-12} . For a BER of 10^{-10} BPSK need 1.8 dBm power in the receiver to be received as signal power whereas OOK needs 4.9 dBm received power to maintain the BER value.

From *Figure 4-6*, it is also clearly evident that BPSK and QPSK gives better performance than other modulation technique in terms of BER vs. average required received power. Among the four modulation techniques, the average BER of BPSK is consistently lower. The BER performance of any modulation scheme cannot be the only metric to measure the performance of a modulation scheme. Bandwidth efficiency is also another prime metrics to evaluate the performance of a modulation technique.

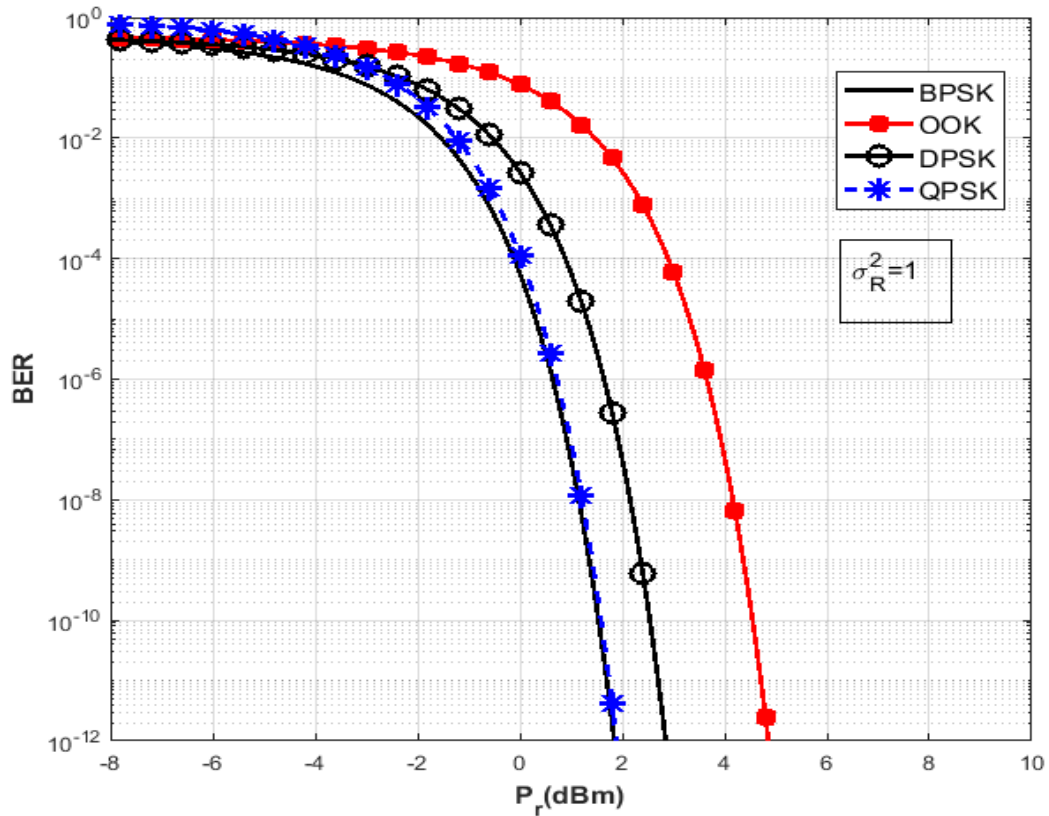


Figure 4-6: Plots of BER vs. Received optical power for different modulation techniques

Figure 4-7 represents the Bit rate vs. Bandwidth curve of the four modulation

techniques. For OOK, BPSK and DPSK schemes, bandwidth efficiency ($\eta_b = \frac{R_b}{B}$) is

1. QPSK is very spectrally efficient since each carrier phase represents two bits of data. Bandwidth efficiency of QPSK is 2. On the other hand, Bandwidth efficiency of OOK, BPSK, DPSK are 1.

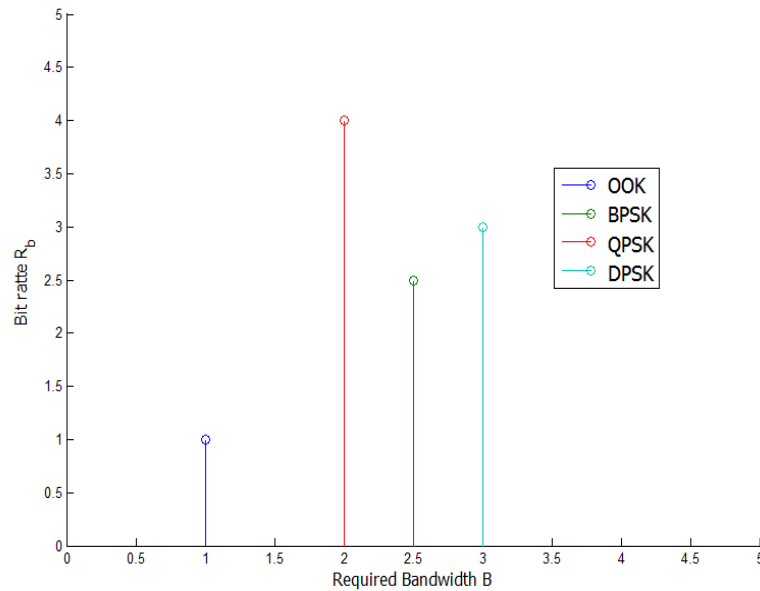


Figure 4-7: Bit rate vs. Bandwidth for different modulation techniques

If we take power efficiency and spectral efficiency both into account, QPSK and BPSK performed far better than other modulations. *Figure.4-8* shows the BER performance of BPSK and QPSK for different levels of scintillation. The power requirement for QPSK is slightly higher than BPSK. It can also be inferred that the BER performance suffers a dramatic degradation with the increase of turbulence strength. For a BER of 10^{-3} the SNR values will be 14.12 dB, 23.46 dB and 38.91 dB for the value of Rytov variance (σ_R^2) 0.4,3,8 respectively. The systems experience a deterioration of BER performance.

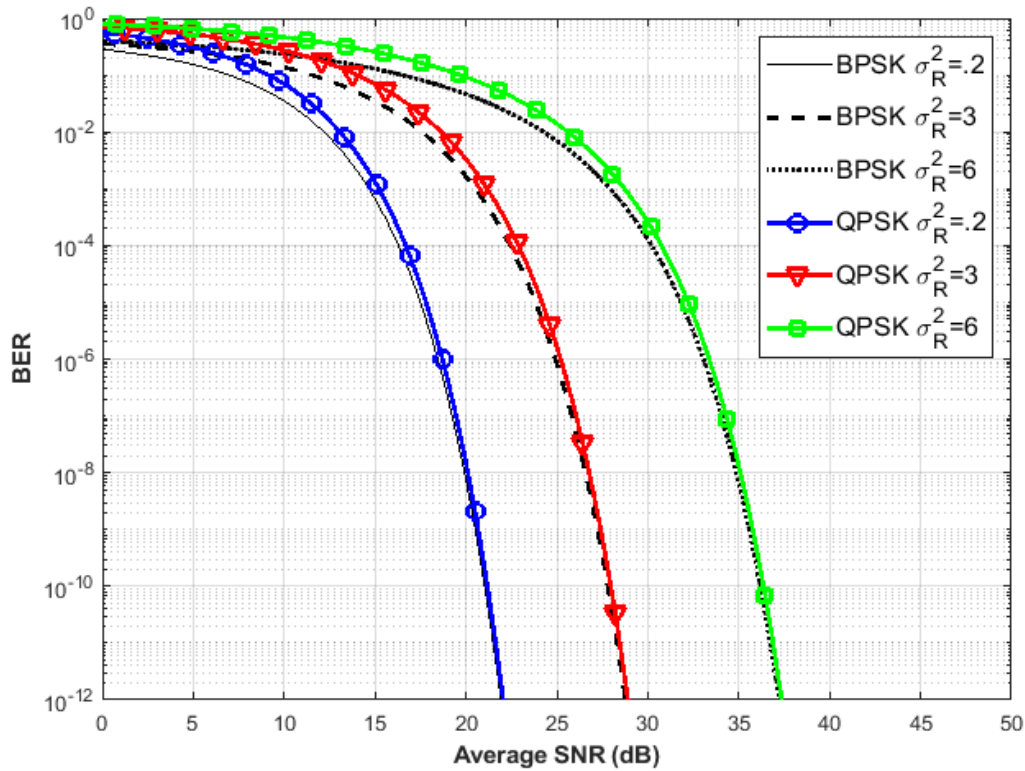


Figure 4-8: Plots of BER vs average SNR for BPSK and QPSK for different turbulence strengths.

In *Figure 4-9*, the coherent FSO system BPSK scheme is simulated for different levels of turbulence. For different values of Rytov variance (σ_R^2 , i.e., 0.4, 1, 3, 6), the SNR values found to be 21.4dB, 23.7dB, 27.6dB and 40.5dB for keeping the BER value 10^{-10} . Higher the value of σ_R^2 , the more power is needed to achieve the same BER performance.

Figure 4-10 in the next page represents the BER and received power curve of the system for BPSK scheme with different turbulence strength. It shows that more the strength of the turbulence more the required received power needed to maintain the same BER value. The system is also robust to both weak and strong turbulence regime. There is a 4dBm difference between the received power of BPSK between the weak turbulence (σ_R^2) and strong turbulence (σ_R^2) regime for a BER of 10^{-12} .

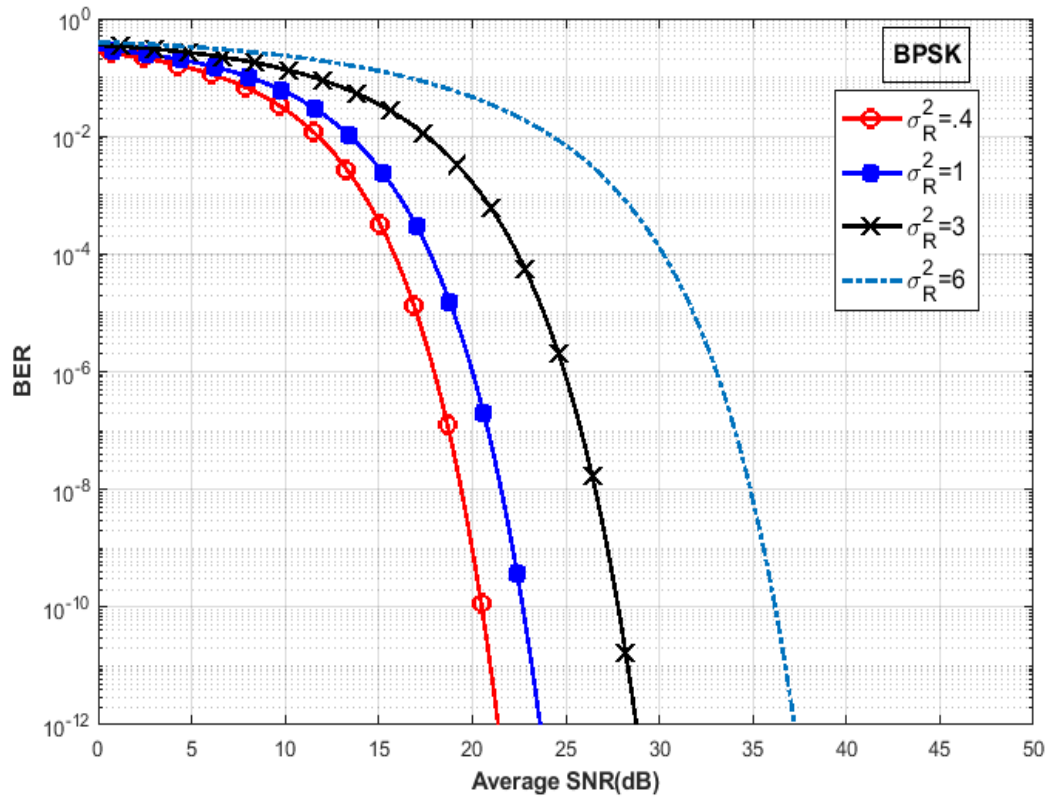


Figure 4-9: BER performance of BPSK for different turbulence strengths.

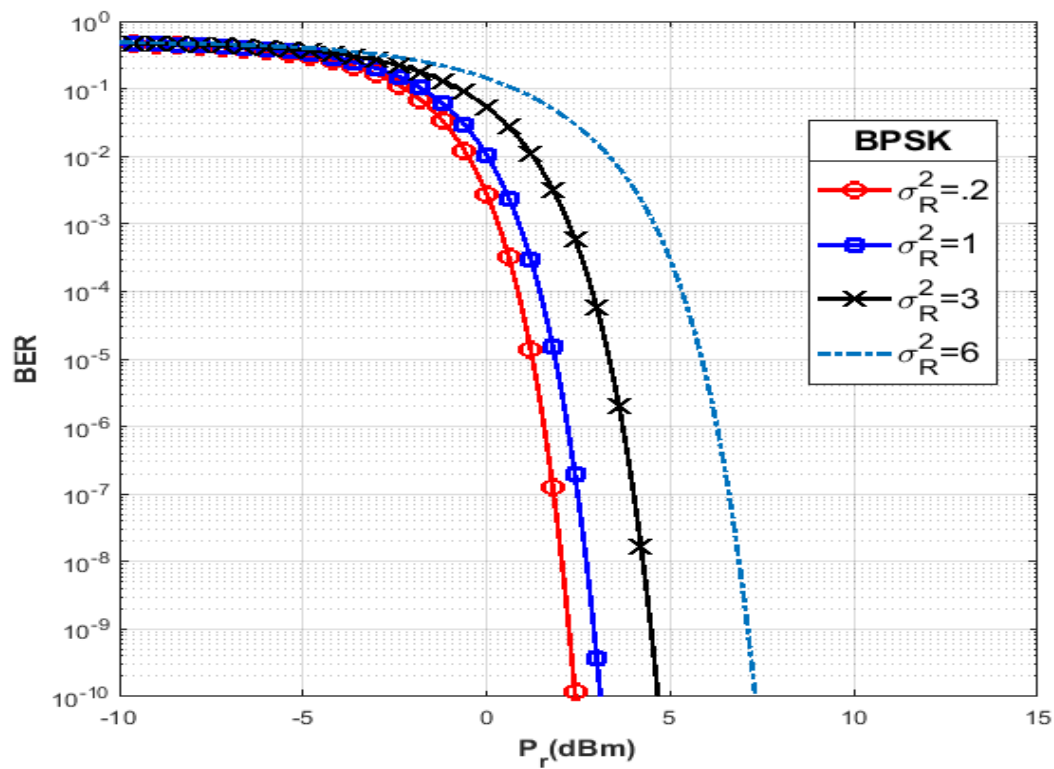


Figure 4-10: Plots of BER vs Received optical power for BPSK for different turbulence strengths.

We can generate the value of Rytov variance by varying the link length and Refractive index structure parameter in equation (70) for our proposed coherent FSO system.

Table 4-2: Values of Rytov variance for different link length (L) for a fixed $C_n^2=10^{-13}m^{-2/3}$

L	300m	700m	1000m	1250m	1850m
σ_R^2	0.2112	1.0046	2.0107	3.0080	6.0112

Figure 4-11 represents the BER vs. SNR graph of the proposed coherent system with BPSK scheme for different link length as well as turbulence strength. It shows that with increase of the value of σ_R^2 more power is needed to maintain the same BER. The system gives similar performance as the system was analyzed previously for a constant σ_R^2 value. For a fixed BER of 10^{-4} , the average SNR on the receiver side for 300m, 1000m and 1850m link length are 16.23dB, 20.12dB and 32.13 dB respectively. It is clearly evident that with the increase in link length the average required received power increases.

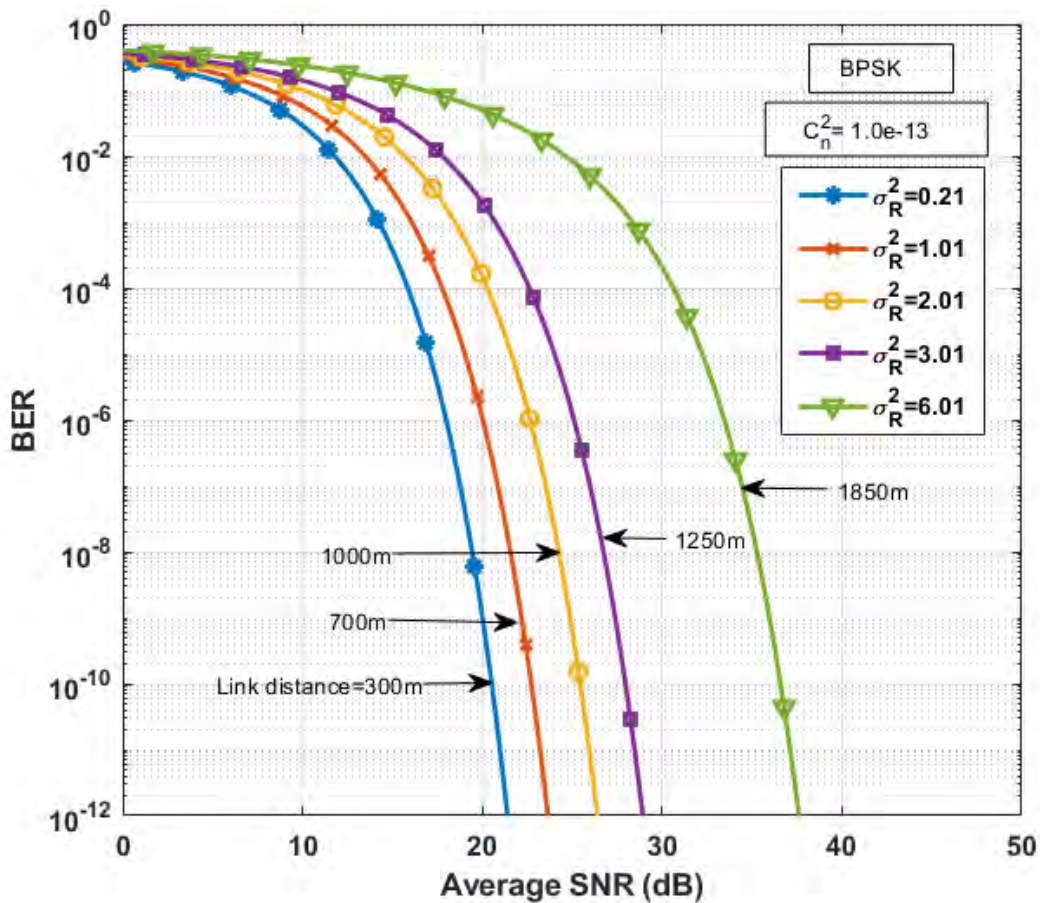


Figure 4-11: BER performance of BPSK for different values of Rytov variances and link distances.

The link length is assumed fixed ($L=1000\text{m}$) and different Rytov variance values are generated by varying the refractive index structure parameter in equation (70).

Table 4-3: Values of Rytov variance for different C_n^2 and link length (L) =1000m

C_n^2	10^{-14}	5.0×10^{-14}	10^{-13}	1.52×10^{-13}	3.0×10^{-13}
σ_R^2	0.1983	0.99	1.98	3.02	5.95

Figure 4-12 represents the BER vs. SNR graph of the proposed coherent system with BPSK scheme for different refractive index structure values with a fixed link length of 1000m. For a fixed BER of 10^{-4} , the average SNR on the receiver side are 15.23dB, 18.52dB and 22.13 dB for the value of Rytov variance 0.19, 0.99 and 1.98 respectively. It is clearly evident that with the increase in turbulence strength the average required received power increases.

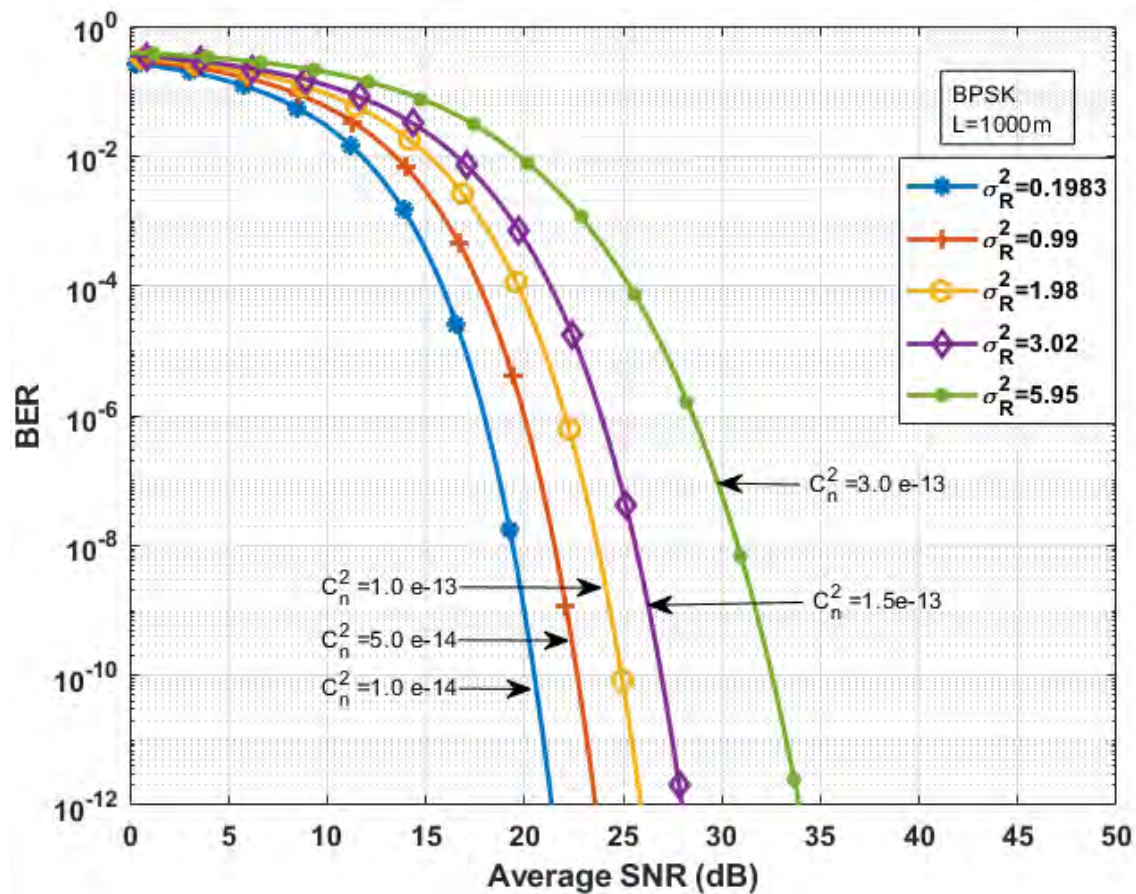


Figure 4-12: BER performance of BPSK for fixed link distance and different values of Rytov variances.

4.4 Comparison of the proposed FSO system with other FSO system

In this section, the BER performance of coherent FSO is compared with a IM/DD FSO system [33], a FSO system with phase modulation techniques [35] and a coherent FSO system with BPSK modulation scheme[40].

Table 4-4: Comparison Table of theproposed coherent FSO system with other systems.

Metric	IM/DD FSO system [42]	FSO system with phase modulation technique [40]	A coherent FSO system with BPSK [46]	Proposed coherent FSO System	
Modulation Technique	OOK	BPSK	BPSK	BPSK	
Wavelength	1550nm	1550nm	1550nm	1550nm	
Photodiode used	APD	Pin	Pin	Pin	
Responsivity	1	1	0.85	0.85	
Link Length	1000m	1000m	-	1000m	
Rytov variance (σ_R^2)	0.8	1	-	1	
(α, β)	-	-	(4, 4)	(4.1,2.5)	
BER	$4*10^{-3}$	10^{-10}	10^{-3}	10^{-3}	10^{-10}
SNR (dB)	18	21.8	20	15.97	20.3

4.5 Summary

The results presented in this chapter indicate that the coherent FSO system gives better performance if BPSK modulation scheme is used. The system achieved better BER vs.SNR performance as well as the requirement of receiver power becomes less when BPSK modulation scheme is incorporated. Therefore, BPSK is a promising modulation format for a FSO communication system considering coherent detection.

CHAPTER 5

CONCLUSION AND FUTURE WORK

5.1 Overview

A coherent FSO system's performance with different modulation schemes has been presented in this thesis. Different components of a FSO system, different modulation schemes and detection techniques have been described in different chapters.

FSO communication nowadays, have attracted considerable research interests due to the limitations of the fiber optic constraints imposed by the nonlinear effects. Significant amount of research works are reported recently on FSO communication system taking into account the limitations imposed by the free-space link such as atmospheric turbulence, pointing error, cloud, fog, rain, etc. As the free space is used as the medium of transmission, the received signal power is reduced due to these effects. When a coherent detection is used, the power received on the receiving side increases as the incoming signal combined with a continuous wave local oscillator's beam before it strikes the photo detector and it results in the rise of receiver's sensitivity as well as BER performance. In this research work, analytical approaches are developed and presented for a coherent system which is analyzed for OOK, DPSK, BPSK and QPSK modulation techniques under various turbulence conditions.

The main contribution of the thesis is the development of analytical model of a coherent FSO system as described in Chapter 4. This chapter will provide concluding remarks in this thesis. The contribution and the implication of the contributions are provided below:

5.2 Summary of the Findings of the Thesis

The main contribution of the thesis is the development of a generalized analytical model of a FSO link with coherent detection where the performance of the four modulation techniques have been analyzed.

Different modulation schemes such as OOK, BPSK, DPSK, QPSK have been incorporated in the coherent FSO system. Currently, most commercially deployed FSO

systems use OOK and Intensity Modulation Direct Detection(IM/DD) scheme whereas in our proposed FSO system, we used coherent detection and analyzed the system for different modulation schemes.

Gamma-gamma model is used for the characterization of the atmospheric channel as this model can be used in both weak and strong turbulence regime.

The best performance has been achieved with both BPSK and QPSK modulation scheme in our proposed system but the BER performance is slightly higher for the BPSK modulation format in our proposed system. For a moderate turbulence condition ($\sigma_R^2=1$), BPSK required 9dBm less SNR than OOK for a BER of 10^{-10} . As atmospheric turbulence is the major reason for the degradation of signal strength in the receiver, a coherent FSO system with an efficient modulation scheme can retrieve a signal with comparatively less BER. Though the practical goal is to achieve a BER of value 10^{-4} , the proposed system demonstrate redundancy upto BER of value 10^{-12} .

5.3 Future Work

In the research work, four modulation technique have been studied. Other kinds of high level modulation scheme: QAM, OFDM-FSO system, etc. can be used in the future to overcome the channel limitations. Also a multipath dispersive channel can be used in near future to have a overall idea of the performance of the system in real-life practical scenario. MIMO, SIMO, MISO, etc; might be incorporated which could give a improved BER vs. SNR performance.

FSO offers many advantages over existing techniques which can be either optical or radio or microwave. Less cost and time to setup are the main attraction of FSO system. Optical equipment can be used in FSO system with some modification. FSO system poses some problem like attenuation in medium that can affect the performance of transmission as power loss would be there. Many studies are going in this perspective to minimize the effect of attenuation by introducing new system design like WDM based FSO system.

Different models based on these studies are used to study the system performance before installing it at the location. This can lead to the improvement of the system. Different

techniques like OFDM-FSO, WDM-FSO based system are new approach to improve the system performance with high speed and longer distance. So, new techniques can be designed by combination of these and by enhancing these techniques, system designing can be improved.

Channel coding can be included in the total calculation of the receiver BER performance, but it might be included in the future work.

Moreover, a multihopping transmission channel can also be incorporated in FSO to impair the channel fading due to the atmospheric channel.

BIBLIOGRAPHY

1. Ghassemlooy Z., Popoola W. and Rajbhandari S., "Optical Wireless Communication", CRC Press, 2013.
2. Chada D., "Terrestrial Optical Wireless Communication", McGrawHill Education, 2013
3. Henniger H. and Wilfert O., "An introduction to free space optical communication", Journal of Radio Engineering, vol.19, no.2, pp.203-212, June 2010.
4. Hamza A. S., Deogun J.S. and Alexander D. R., "Classification Frameworks for Free Space Optical Communication Links and Systems", IEEE Communication Surveys and Tutorials, vol.21, no.2, pp.1346-1382, 2019.
5. Sadiku M.N.O and Musa S.M, "Free Space Optical Communications: An Overview", vol.12, no.9, pp.55-68, 2016.
6. Malik A. and Singh P., "Free Space Optics: Current Applications and Future Challenges", International Journal of Optics, vol.15, pp.1-7, 2015.
7. Khalighi M. A. and Uysal M., "Survey on Free Space Optical Communication: A Communication Theory Perspective", vol.8, no.1, pp.1-29, 2014.
8. Kaur A. and Panchal R. K., "Analysis of effect of atmosphere turbulence in free space optical (FSO) communication system", International Journal of Engineering and Innovative Technology, vol. 3, no.11, pp.301-305, May 2014.
9. Zhang M., Tang X., Lin B., Ghassemlooy Z. and Wei Y., "Analysis of Rytov Variance in Free Space Optical Communication under the weak turbulence", International Conference on Optical Communications and Networks, vol.89, no.1, pp.99-106, 2017.
10. Sing J., Kapoor V. and Kumar N., "Performance evaluation of high speed optical wireless communication system", International Journal of Computer Application, vol.4, no.5, pp.11-14, 2012.
11. Kovachev Y. and Mitsev T., "A Brief Survey of the Methods for Increasing FSO Availability", In-Silico Intellect, vol.1, no.1, 2017.
12. Rathore S. and Rathore D., "Effect of Transmitter Pointing Error Angle on Intersatellite Communication", International Journal of Current Engineering and Technology, vol.5, no.3, pp.1939-1941, 2015.
13. Prokes A., "Modeling of atmospheric turbulence effect on terrestrial FSO link", Journal of Radio Engineering, vol.18, no.1, pp.42-47, 2009
14. Shah D., Nayak B. and Jethawani D., "Study of different atmospheric channel models", International Journal of Electronics and Communication Engineering and Technology, vol.5, no.1, pp.105-112, 2014.
15. Zhu X. and Kahn J.M., "Free-space optical communication through atmospheric turbulence channels", IEEE transactions on communications, vol.50, no.8, pp.1293-1300, August 2002.
16. Andrews L.C. and Phillips R.L., "I-K distribution as a universal propagation model of laser beams in atmospheric turbulence", Journal of Optical Society of America A, vol.2, no.2, pp.160-163, 1985.
17. Clifford S.F and Hill R.J., "Relation between irradiance and log-amplitude variance for optical scintillation described by the K-distribution", Journal of Optical Society of America, vol.71, no.1, pp.112-114, 1981.

18. Popoola W., Ghassemloy Z. and Leitgeb E., "Free Space optical communication using subcarrier modulation in gamma-gamma atmospheric turbulence", 9th International Conference on Transport Optical Network (ICTON'07), Warsaw, Poland, vol.3, pp.156-160, July 2007.
19. Shaina and Gupta A., "Comparative Analysis of Free Space Optical Communication System for Various Optical Transmission Windows under Adverse Weather Conditions", *Procedia Computer Science*, vol.89, no.1, pp.99-106, 2016.
20. Mikolajczyk J. and Bielecki Z., "Analysis of Free-Space Optics Development", *Procedia Computer Science*, vol.24, no.4, pp.653-674, 2017.
21. Sharma D. and Khan S.A., "Literature Survey and Issue on Free Space Optical Communication System", *International Journal of Engineering Research and Technology*, vol.4, no.2, 2015.
22. Senior J.M., "Optical Fiber Communications Principles and Practice", 3rd ed. Essex: Pearson Education Limited, 2009.
23. Hecht J., "Understanding Fiber Optics", 5th ed. Upper Saddle River, New Jersey: Prentice Hall, 2005.
24. Pratt W.k., "Laser Communication Systems", 1st ed. New York: McGraw-Hill Professional, 2003.
25. Keiser G., "Optical Communication Essentials", 1st ed. New York: McGraw-Hill Professional, 2003.
26. Kedar D. and Arnon S., "Urban optical wireless communication networks : the main challenges and possible solutions", *IEEE Communications Magazine*, vol.42, no.5, pp.S2-S7, 2004.
27. Wahab F. A., Zamri N.A. and Leong T. K., "Multiple transmitters and receivers for free space optical communication link performance analysis", *Journal of Telecommunication, Electronic and Computer Engineering*, vol.8, no.5, 2016.
28. Amphawan S., Chaudhary S. and Chan V.W.S., "2x20 Gbps -40 GHz OFDM Ro-FSO transmission with mode division multiplexing", *Journal of European Optical Society: Rapid Publications*, no.9, pp., 2014.
29. Li L., Xie G., et al., "Performance Enhancement of an Orbital-Angular-Momentum-Based Free Space Optical Communication Link through Beam Divergence Controlling", *Optical Fiber Communication Conference, OSA Technical Digest (online)*, 2015.
30. Betti S., De Marchis G. and Iannone E., "Coherent Optical Communication Systems", 1st ed. Toronto, Canada: John Wiley & Sons Inc., 2002.
31. M. Uysal, J. Li, and M. Yu, "Error rate performance analysis of coded free-space optical links over gamma-gamma atmospheric turbulence channels," *IEEE Trans. Wireless Commun.*, vol.5, no.3, pp.1229-1233, 2006.
32. Kim I., Goldfarb G. and Li G., "Electronic wavefront correction for PSK free space", *Electronic Letter* 43, pp.1108-1109, 2007.
33. Kausal H. and Kaddoum G., "Free Space Optical Communication: Challenges and Mitigation Techniques", *IEEE Communications Surveys & Tutorials*, vol.19, no.1, pp.57-96, 2015.
34. Ali M. A. A., "Free Space Optical communication for Different Weather Conditions", vol.23, no.2, pp.81-90, 2012.

35. Zhu X. and Kahn J.M., "Free space optical communication through atmospheric turbulence channel", *IEEE transactions on Communications*, vol.50, no.1, pp.1293-1300, 2002.
36. N. A. Mohammed, A. S. El-Wakeel, and M. H. Aly, "Pointing Error in FSO Link under Different Weather Conditions," *International Journal of Video & Image Processing and Network Security (IJVIPNS-IJENS)*, vol. 12, no.1, pp. 6-9, 2012.
37. Elaganimi T. U., "Performance comparison between OOK, PPM and PAM Modulation schemes for free space optical (FSO) communication", *International Journal of Computer Applications*, vol.79, no.11, pp.22-27, 2013.
38. Islam A.K.M.N and Majumdar S.P, "Effect of timing jitter on the BER Performance of a M-PPM FSO Link over Atmospheric Turbulence Channel", *Proceedings of International Conference on Electrical and Computer Engineering*, pp.409-412, 2014.
39. Wang Z., Zhong W. D., Fu S., Lin C., "Performance comparison of different modulation formats over free space optical (FSO) turbulence links with space diversity reception technique", vol.1, no.6, pp.277-285, 2009.
40. Zhang H., Li H., Dongya X. and Chao C., "Performance analysis of different modulation techniques for free-space optical communication system", *Telkomnica*, vol.13, no.3, pp.880-888, September 2015.
41. Singh H. and Arora M., "Comparison of bit error rate performance of different modulation technique over turbulent FSO link", *International Journal of Computer Applications*, vol.109, no.12, pp.20-24, 2015.
42. Milica I. Pethovic, Goran T. Dordevic C, Dejan and N. Milic, "BER performance of IM/DD FSO system with OOK using APD receiver", *Journal of Radio Engineering*, vol.23, no.1, pp.480-487, 2014.
43. Kiasaleh K., "Performance of APD based, PPM free space optical communication systems in atmospheric turbulence", *IEEE Transactions on Communications*, vol.53, no. 9, pp.1455-1461, 2005.
44. Tsiftsis T. A., "Performance of heterodyne wireless optical communication system over Gamma-Gamma atmospheric turbulence channels", vol. 44, no.5, pp.372-373, *Electronic Letters*, 2008.
45. Zhang M., Tang X., Lin B., Ghassemlooy Z. and Wei Y., "Analysis of Rytov Variance in Free Space Optical Communication under the weak turbulence", *International Conference on Optical Communications and Networks*, vol.89, no.1, pp.99-106, 2017.
46. Lim W., "BER analysis of coherent free space optical systems with BPSK over Gamma-Gamma Channels", *Journal of the Optical Society of Korea*, vol.19, no.3, pp. 237-240, June 2015.